nature microbiology

Article

https://doi.org/10.1038/s41564-025-02155-9

Engineered *Metarhizium* fungi produce longifolene to attract and kill mosquitoes

Received: 4 April 2025

Accepted: 17 September 2025

Published online: 24 October 2025

Check for updates

Dan Tang[1,6], Jiani Chen[2,6], Yubo Zhang[1,6], Xingyuan Tang[1], Xinmiao Wang[1], Chaonan Yu[1], Xianxian Cheng[1], Junwei Zhang[2], Wenqi Shi[2], Qing Zhen[1], Shuxing Liu[1], Yizhou Huang[1], Jiali Ning[1], Guoding Zhu[3], Meichun Zhang[3], Jubing Hu[3], Etienne Bilgo[4], Abdoulaye Diabate[4], Sheng-Hua Ying[1], Jun Cao[3] ✉, Raymond J. St. Leger[5] ✉, Jianhua Huang[2] ✉ & Weiguo Fang[1] ✉

Chemical insecticides have been the primary method of mosquito control, but in recent years, mosquitoes have become resistant to these compounds. *Metarhizium* fungi are emerging as promising alternatives and can kill mosquitoes with a small number of spores. It was previously shown that caterpillars affected by fungal infections can attract mosquitoes. However, the mechanisms and potential applications of this attraction are lacking. Here we show that *Metarhizium*-colonized insect cadavers release the volatile longifolene to attract and infect healthy insects, facilitating spore dispersal. We identified the responsible odorant receptors in *Drosophila melanogaster* and *Aedes albopictus*. The virulent mosquito pathogen *Metarhizium pingshaense* was engineered to express pine longifolene synthase to produce a large amount of longifolene on media. The transgenic spores effectively attracted and killed male and female *A. albopictus*, *Anopheles sinensis* and *Culex pipiens*. Attraction of wild-caught mosquitoes was not impacted by human presence, but mosquito-attracting flowering plants competed with transgenic *M. pingshaense* for attractiveness, although mortality remained over 90%. This study uncovered an active spore dispersal mechanism in broad-host-range entomopathogenic *Metarhizium*, enhancing mosquito control efficacy.

Mosquitoes are the most dangerous animals on earth, with an estimated two billion people at risk of serious mosquito-borne diseases including malaria, dengue and chikungunya. Chemical insecticides have been the primary method of mosquito control, but mosquitoes have gained sufficient resistance to render insecticides ineffective[1]. *Metarhizium* fungi are emerging as promising alternatives owing to their eco-friendly nature and efficacy against insecticide-resistant mosquitoes, even increasing their susceptibility to chemical insecticides[2,3].

The effectiveness of *Metarhizium* is largely contingent upon the infection rate, as some *Metarhizium pingshaense* strains can kill mosquitoes with a small number of spores[3]. Typically, *Metarhizium* spores are applied with external physical or chemical cues that attract mosquitoes. Previous semi-field trials used spores in an oil formulation applied to mosquito-attractive black cloth. This control method achieves a substantial infection rate (~75%) only for indoor blood-fed female mosquitoes[4], and it is unsuitable for outdoor mosquito control.

Mosquitoes use olfactory cues for host seeking, nectar foraging and oviposition, which can be exploited to attract them into traps. However, current mosquito traps are costly and unwieldy, requiring multiple commercial attractants for efficacy[5]. This has restricted their use with fungi, despite host attractants increasing the transmission of *Metarhizium* spores[6]. In nature, *Metarhizium* spores are generally

A full list of affiliations appears at the end of the paper. ✉e-mail: caojuncn@hotmail.com; stleger@umd.edu; jhhuang@zju.edu.cn; wfang1@zju.edu.cn

assumed to disperse through random insect contact or environmental factors such as rainfall[7]. However, laboratory observations of mycosed caterpillars attracting mosquitoes[8] have opened new possibilities regarding the ecology of these ubiquitous fungi and trap design. However, comprehensive studies exploring the mechanisms and potential applications of this attraction are lacking.

Here we report that insect cadavers colonized by *Metarhizium robertsii*, a model species for investigating *Metarhizium* biology[9], emit volatiles, including the common plant volatile longifolene, which attract diverse insect taxa, facilitating the dissemination of this broad-host-range pathogen across multiple species. The study identified the receptors in *Drosophila melanogaster* and *Aedes albopictus* attuned to *M. robertsii*-infested-cadaver odours. Based on this, a strain of *M. pingshaense*, a virulent mosquito pathogen, was engineered to have attractive spores that can be mass produced using inexpensive media. These spores serve as both lure and mycoinsecticide, effectively eliminating mosquitoes.

Results

M. robertsii-colonized insect cadavers attract diverse insect taxa

While assaying *M. robertsii*'s virulence against *Galleria mellonella* larvae, we noticed that healthy larvae were attracted to mycelium-covered cadavers. To investigate whether the colonized cadavers could attract other insects and explore the pest control potential of this phenomenon (Supplementary Fig. 1), we conducted two-choice assays to investigate the responses of several phylogenetically distant insect pests or natural enemies to the cadavers versus freeze-killed healthy *G. mellonella* larvae. The colonized cadavers attracted *G. mellonella* larvae (Lepidoptera), adult and larval *D. melanogaster* (Supplementary Video 1), adult *A. albopictus* mosquitoes (Diptera), adult wasp *Leptopilina boulardi* (Hymenoptera), and adult cotton mealybug *Phenacoccus solenopsis* and whitefly *Bemisia tabaci* (Homoptera) (Fig. 1a).

M. robertsii colonizing insect cadavers dispersed via infection and defecation by attracted insects

We used the strain WT-GFP, expressing green fluorescent protein (GFP) in *M. robertsii* (Extended Data Fig. 1a), to track spores picked up by healthy insects after exposure to WT-GFP-colonized *G. mellonella* cadavers. Spores were transferred to the cuticle of all attracted insects. Spores were also found in the alimentary canals of insects ingesting solid food, including *G. mellonella* and *D. melanogaster* larvae (Extended Data Fig. 1b). Almost all *G. mellonella* larvae died from WT-GFP infection within 12 days post-exposure and transformed into mycosed cadavers (Fig. 1b).

We investigated the fate of ingested spores using *G. mellonella* larvae, as their comparatively large size facilitated these studies. During exposure, the larvae consumed *M. robertsii*-colonized *G. mellonella* cadavers (Fig. 1b). After 30 min of exposure and following body surface sterilization, spores remaining attached on intersegmental membranes were dead as no WT-GFP colonies appeared on *Metarhizium*-selective medium inoculated with the sterilized cuticles (Extended Data Fig. 1c). Ungerminated WT-GFP spores were observed in the faeces of the cleaned insects, confirming gut passage (Fig. 1c). Spore viability was verified by the appearance of WT-GFP colonies on selective medium inoculated with faecal suspensions (Fig. 1c). Although the number of WT-GFP colonies decreased over time, viable spores were still found in faeces 6 days post-exposure (Fig. 1c), indicating the potential for environmental dispersal in faeces. Approximately 70% of the surface-sterilized larvae died from WT-GFP infections (Fig. 1b). We examined whether ingested spores caused this mortality. WT-GFP spores were observed in all gut sections 2 days post-exposure, but had only germinated in the foreguts (Extended Data Fig. 1d). By 72 h, hyphae had penetrated the oesophagus and crop areas of the foreguts (Fig. 1d). After 96 h, the haemocoel was populated with WT-GFP blastospores (Extended Data Fig. 1d).

M. robertsii-colonized insect cadavers emit longifolene to attract insects

We sought to identify which insect-attracting volatiles were emitted from *M. robertsii*-colonized *G. mellonella* cadavers over extended periods to develop fungal strains with long-term mosquito attraction and killing abilities. We distinguished between (1) cadavers without emerged mycelia within 1 day after death (1-day cadavers), (2) cadavers covered with sporulating mycelia 6 days after death (6-day cadavers) and (3) fully sporulated mycelia that had ceased sporulation (12-day cadavers) (Fig. 2a). The 12-day cadavers were maintained at room temperature to produce 30–100-day cadavers. Two-choice assays showed that 1-day cadavers were not attractive to *D. melanogaster* larvae, while cadavers aged 6 days and older were equally attractive (Fig. 2a). We found that three volatile organic compounds (VOCs), (+)-longifolene (Chemical Abstracts Service (CAS): 475-20-7), (+)-sativene (CAS: 3650-28-0) and (−)-geosmin (CAS: 19700-21-1), were persistently emitted by the cadavers aged 6 days and older, but not detected in 1-day cadavers and freeze-killed healthy *G. mellonella* larvae (Fig. 2b,c). Their retention indices on non-polar and polar gas chromatography (GC) columns matched their respective authentic standards (Supplementary Table 1) and were very similar (>99.6%) to published indices[10,11]. The 50-day cadavers produced approximately 3-fold more longifolene (0.9 ng g^{-1} cadaver per h) than younger cadavers ($P < 0.05$, one-way ANOVA with Tukey's multiple-comparison test, $n = 3$), and this level remained high (Fig. 2c). Sativene and geosmin levels peaked in the new cadavers and then decreased (Fig. 2c). Spore lipid droplets isolated from 12-day cadavers were attractive to *D. melanogaster* larvae and contained longifolene, sativene and geosmin (Fig. 2b and Supplementary Results).

Two-choice assays (mycelia versus cotton) showed that sporulated mycelia (0.05 g) separated from 12-day cadavers attracted *D. melanogaster* larvae, whereas the same amounts of sporulated mycelia from potato dextrose agar (PDA) or non-sporulated mycelia from liquid Sabouraud dextrose broth supplemented with yeast (SDY) did not (Fig. 2d). Two-choice assays (the three types of mycelia versus each other) showed that cadaver mycelia were more attractive than PDA and SDY, and PDA mycelia were more attractive than SDY ($P < 0.05$, two-tailed Student's t-test, $n = 6$) (Fig. 2d). Even at the weight (0.4 g) of single colonized cadavers, SDY mycelia remained unattractive, whereas PDA mycelia were attractive (Fig. 2e). The cadaver mycelia emitted 2-fold more longifolene (1.4 ng g^{-1} mycelium per h) than PDA, but both released similar amounts of sativene and geosmin (Fig. 2d). SDY mycelia emitted only geosmin (Fig. 2d). These emission differences implicate longifolene, preferentially expressed by cadavers, in the attractiveness of *M. robertsii*-colonized cadavers.

Two-way choice assays (longifolene versus the blank control hexane) showed that longifolene was indeed attractive to *D. melanogaster* larvae in a dose-dependent manner within 10^{-11}–10^{-5} g (Fig. 3a). The amount of longifolene released by single *M. robertsii*-colonized *G. mellonella* cadavers aged 6 days and older was within this range (Fig. 2c).

Longifolene receptors in *D. melanogaster* larvae

D. melanogaster larvae of *Orco*[2], a mutant in the *Orco* gene encoding an obligate co-receptor of all odorant receptors (OR)[12], did not respond to longifolene (Fig. 3b), confirming olfaction's role in attraction. To identify larval longifolene receptors, deficiency lines of 21 larval ORs and Orco were constructed using the Or-GAL4/UAS-tetanus toxin light chain (UAS-TNT) system[13]. Similar to the Orco-deficient line, neither Or43b- nor Or74a-deficient lines responded to longifolene (Fig. 3b), while the other 19 Or-deficient lines showed no difference from the WT (wild type) (Extended Data Fig. 2). To validate these results, the *Or43b* mutant $Or43b^{l4}$ and the *Or74a* mutant $Or74a^{D31}$ were constructed using clustered regularly interspaced short palindromic repeats (CRISPR)–CRISPR-associated protein 9 (Cas9) (Extended Data Fig. 3). A reported *Or43b* mutant $Or43b^{1.w-}$ (ref. 14), was also included. Larvae of *Or43b* and *Or74a* mutants were not attracted to longifolene (Fig. 3b).

https://doi.org/10.1038/s41564-025-02155-9

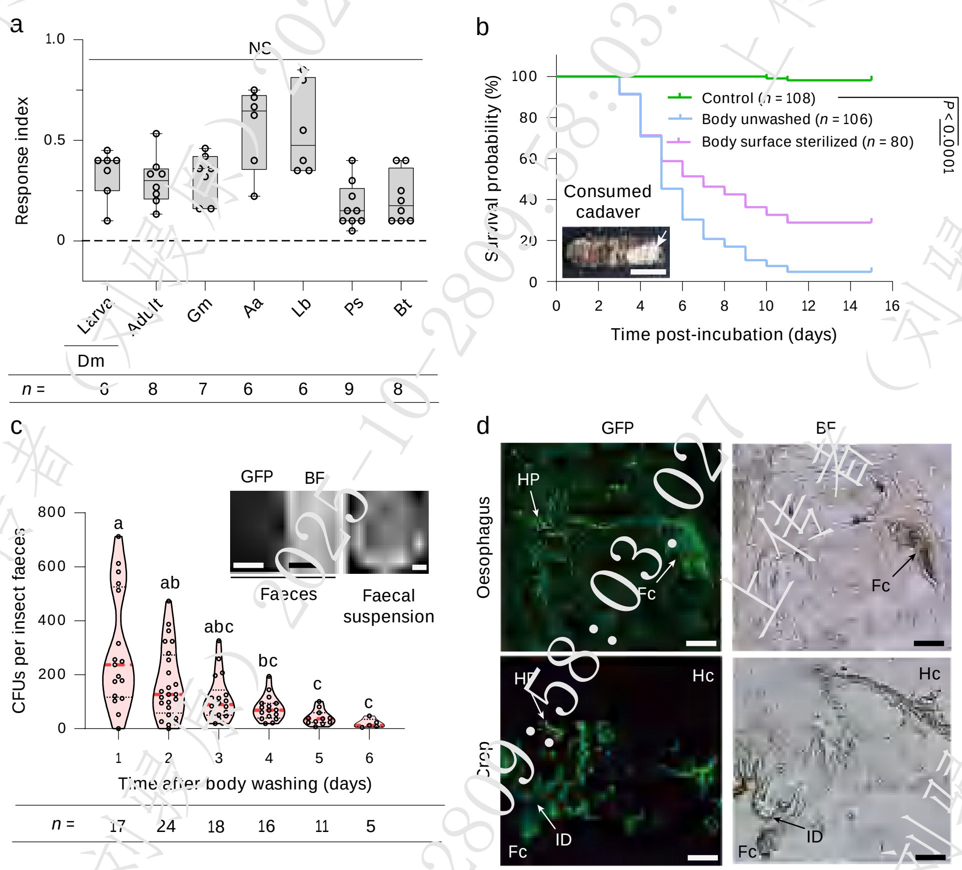

Fig. 1 | *M. robertsii*-colonized cadavers attract healthy insects for active spore dispersal. a, Two-way choice or two-port olfactometer assays of response (shown as response index) of six insect species to *M. robertsii*-colonized *G. mellonella* larval cadavers versus freeze-killed healthy *G. mellonella* larvae (uninfected control cadavers). The response index was calculated as $(O - C)/T$, where O was the number of larvae in the mycosed cadaver zone, C was the number in the uninfected control cadaver zone and T was the total number of insects assayed; this calculation was applied in all similar assays below. n, experiment repeats. The box plots show the median (centre line), the interquartile range (box bounds, 25th to 75th percentiles) and the minima and maxima (whiskers) within 1.5× interquartile range from the box. Dm, *D. melanogaster*; Gm, *G. mellonella* larvae; Aa, *A. albopictus* adult females; Ps, *P. solenopsis* adults; Bt, *B. tabaci* adults; Lb, *L. boulardi* adults. NS, not significantly different ($P > 0.05$, Kruskal–Wallis test with Dunn's multiple-comparison test). **b**, Kaplan–Meier curves of survival of *G. mellonella* larvae after 30 min of exposure to the cadavers. Inset: a cadaver with a part bitten off (arrow) by healthy larvae (scale bar, 1 cm). Log-rank test was used (n, the number of insects assayed). **c**, CFU counts in faeces produced by individual *G. mellonella* larvae after 30 min of exposure to the cadavers. Horizontal line, median; n, the number of insects assayed. Values with different letters are significantly different ($P < 0.05$, one-way ANOVA with Tukey's multiple-comparison test). Faeces inset (scale bars, 10 μm), GFP-labelled spores in faeces under epifluorescence (GFP) or bright-field (BF) microscopy; faecal suspension inset (scale bar, 1 cm), *Metarhizium*-selective medium inoculated with faecal suspension and incubated for 5 days at 26 °C. **d**, Gut sections of a *G. mellonella* larvae that ingested spores showing penetration of the foregut (crop and oesophagus). GFP-labelled fungi in sliced (15 μm) foregut, 72 h post-exposure and body sterilization, under epifluorescence (left) or BF (right) microscopy. Scale bars, 50 μm. Images are representative of at least three independent experiments. HP, hyphae; Hc, haemocoel; ID, intima dentation; Fc, foregut cavity.

For single sensillum recording (SSR) assays, Or43b and Or74a were ectopically expressed in the olfactory receptor neurons (ORNs) within T1 trichoid sensilla on *D. melanogaster* antennae. Expression of either receptor conferred spontaneous spikes to the T1 ORNs, indicating correct folding and localization (Supplementary Fig. 2). When challenged with longifolene, both Or43b- and Or74a-expressing neurons showed robust responses in a dose-dependent manner; at each dosage, the response of the Or43b-expressing neuron was stronger than that of the Or74a-expressing neuron ($P < 0.001$, two-tailed Student's t-test, $n = 10$) (Fig. 3c,d).

Contribution of longifolene to the attractiveness of *M. robertsii*-colonized insect cadavers

In contrast to the WT, *Orco*[2] larvae did not respond to 12-day cadavers (Supplementary Video 2), which were not significantly different from *Or74a* and *Or43b* mutants ($P > 0.05$, one-way ANOVA with Tukey's multiple-comparison test, $n = 10$) (Fig. 3e). Consistently, *M. robertsii* caused 70% mortality of WT larvae, 3.1-fold greater than that of *Orco*[2] (22.5%) ($P < 0.01$, one-way ANOVA with Tukey's multiple-comparison test, $n = 10$), with no difference among *Orco*[2], *Or43b* and *Or74a* mutants ($P > 0.05$) (Fig. 3e).

Both Or74a and Or43b were expressed in larvae, and Or43b was also expressed in adult antennae (Extended Data Fig. 4 and Supplementary Results). Gas chromatography–electroantennographic detection (GC–EAD) showed that longifolene elicited antennal response in both sexes of *D. melanogaster* adults (Fig. 3f). Electroantennography (EAG) assays revealed a strong dose-dependent response to longifolene in the WT and *Or74a* mutant antennae, which was significantly greater than that in *Or43b* mutants ($P < 0.001$, one-way ANOVA with Tukey's multiple-comparison test, $n = 10$) (Fig. 3g). The response of the *Or43b* mutants was significantly stronger than that of the *Orco*[2] mutants ($P < 0.05$) (Fig. 3g), suggesting that other unidentified ORs could be also involved in the adult response. Compared with *Or74a* mutants and WT adults, *Or43b* and *Orco*[2] mutants had significantly reduced responses to longifolene ($P < 0.01$, one-way ANOVA with Tukey's multiple-comparison test), with no difference between the latter two ($P > 0.05$) (Fig. 3h), suggesting that Or43b has a major role in adult behavioural responses to longifolene. Consistently, the *Or74a*

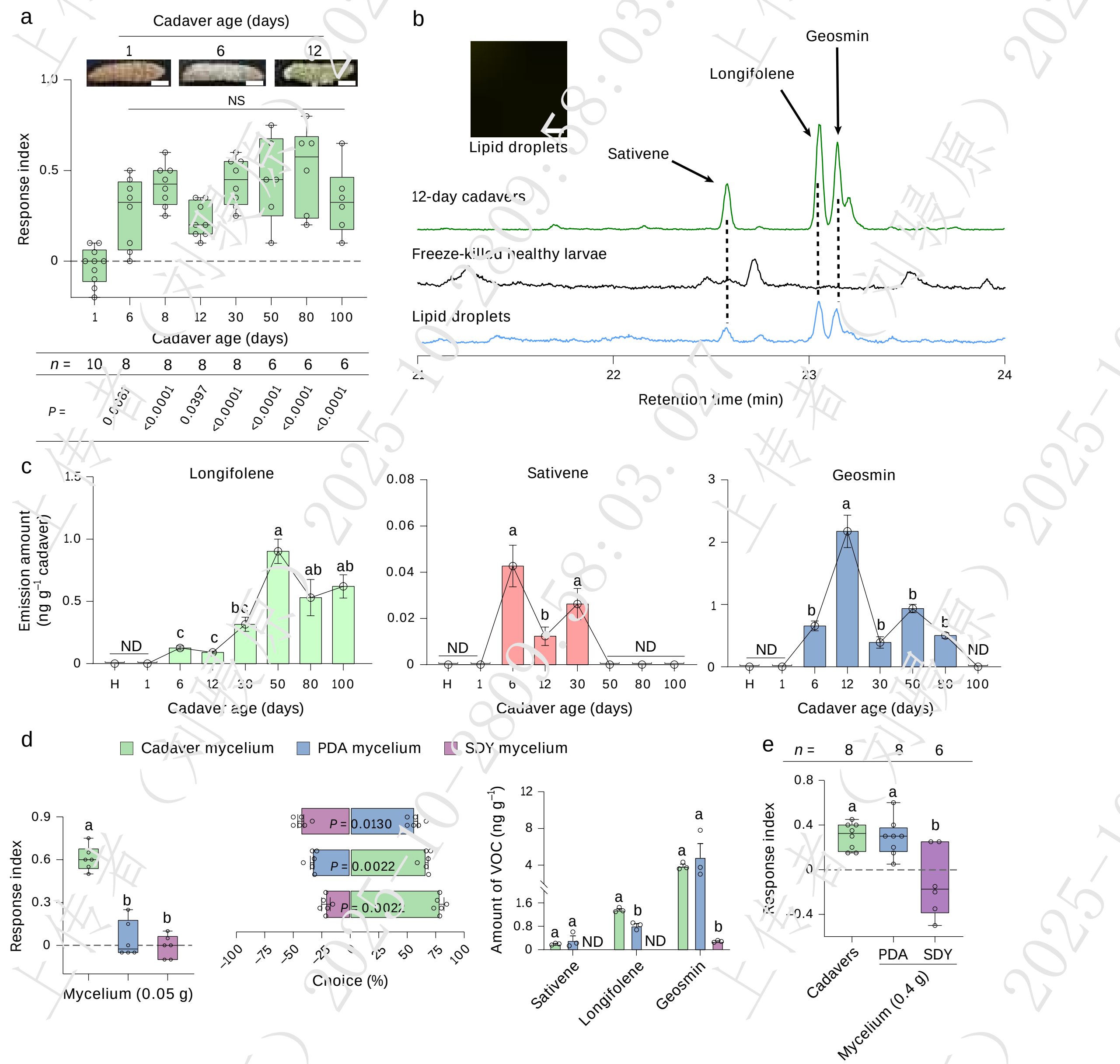

Fig. 2 | Identification of VOCs persistently emitted by *M. robertsii*-colonized *G. mellonella* cadavers. a, Two-way choice assays of *D. melanogaster* larvae response to the mycosed cadavers of different ages (each versus freeze-killed healthy *G. mellonella* larvae). The box plots show the median (centre line), the interquartile range (box bounds, 25th to 75th percentiles), and the minima and maxima within 1.5× interquartile range from the box (whiskers) (used for the response index in **d** and **e** of this figure). *P* values are for comparisons of 1-day cadavers with each of the cadavers aged 6 days or older (two-tailed Student's *t*-test). NS, not significantly different among cadavers aged 6 days and older ($P > 0.05$, one-way ANOVA with Tukey's multiple-comparison test). *n*, experiment repeats. Inset: representative images (of at least 10 cadavers) of 1-day, 6-day and 12-day cadavers. Note: there were no obvious morphologic differences among sporulated mycelium-covered cadavers aged 12 days and older. Scale bars, 1 cm. **b**, GC analysis of three persistently emitted VOCs (longifolene, sativene and geosmin). Lipid droplets (inset: representative image of three independent experiments) were prepared from spores collected from 12-day cadavers (scale bar, 10 µm). **c**, Emission of longifolene, sativene and geosmin by the mycosed cadavers of different ages and freeze-killed *G. mellonella* healthy larvae (H). For each VOC, values with different letters are significantly different ($P < 0.05$, one-way ANOVA with Tukey's multiple-comparison test, $n = 3$). Data are presented as mean ± s.e. ND, not detectable. **d**, Attraction to *D. melanogaster* larvae of mycelia (0.05 g) separated from 12-day cadavers, and PDA and SDY medium. Left: two-choice assays of *D. melanogaster* larvae response to mycelium versus water-soaked cotton. Values with different letters are significantly different ($P < 0.01$, Kruskal–Wallis test with Dunn's multiple-comparison test, $n = 6$). Middle: two-choice assays of behavioural preferences of *D. melanogaster* larvae for the three types of mycelia. Behavioural preference was shown as the percentage of insects in either stimulus zone out of the total number of insects that had made a choice, which was calculated as N1 or N2/(N1 + N2), where N1 was the number of insects in the stimulus 1 zone and N2 was the number in the stimulus 2 zone; this calculation was applied in all similar assays below. Data are presented as mean ± s.e. Two-tailed Student's *t*-test was used ($n = 6$). Right: amounts of longifolene, sativene and geosmin released by the three types of mycelia. Within each VOC, data with different letters are significantly different ($P < 0.05$, one-way ANOVA with Tukey's multiple-comparison test, $n = 3$). Data are presented as mean ± s.e. **e**, Two-choice assays (mycelia versus water-soaked cotton) of *D. melanogaster* larvae responses to PDA or SDY mycelium (0.4 g) or single mycosed cadavers (~0.4 g). Values with different letters are significantly different ($P < 0.05$, one-way ANOVA with Tukey's multiple-comparison test). *n*, experiment repeats.

mutant and WT adults were equally attracted to *M. robertsii*-colonized *G. mellonella* cadavers, while *Or43b* and *Orco*^{2} mutants did not respond (Fig. 3i). No sex-related differences in responses to longifolene and the cadavers were found (Fig. 3g–i).

Characterization of mosquitoes' response to longifolene

We further investigated whether longifolene is also a mosquito attractant. Two-port olfactometer assays (longifolene versus hexane) showed that longifolene was attractive to both sexes of adult *A. albopictus* mosquitoes in a dose-dependent manner (Fig. 4a). GC–EAD assays confirmed that longifolene elicited antennal responses (Fig. 3f). Similar to the mosquito attractant 1-octen-3-ol (ref. 15), EAG assays showed a dose-dependent antennal response to longifolene (Fig. 4b).

Basic Local Alignment Search Tool (BLAST) showed that orthologues of *D. melanogaster* longifolene receptor Or43b were present in *Aedes* (XP_029725568.1 (GenBank accession number), $8 \times e^{-10}$), *Anopheles* (KFB407327, $1 \times e^{-8}$) and *Culex* (XP_039453526, $2 \times e^{-7}$) mosquitoes and other insects including the wasp *L. boulardi* (XP_051167897, $2 \times e^{-8}$) and the blowfly *Calliphora stygia* (AID61209, $6 \times e^{-72}$). No orthologues of another *D. melanogaster* longifolene receptor Or74a were found in mosquitoes, but they were found in other insects including *C. stygia* (AID61223, $6 \times e^{-124}$) and *Lutzomyia longipalpis* (XP_055683865, $1 \times e^{-11}$).

We then assayed whether orthologues of *D. melanogaster* Or43b were longifolene receptors in *A. albopictus*. Double-stranded RNA (dsRNA) injections were conducted to knock down the expression of the *Orco* gene (XP_029733114.1) and three *Or43b* homologous genes (*LOR* (longifolene receptor; see below), XP_029725568; *POR1* (putative OR 1), XP_062713057; *POR2* (putative OR 2), XP_019530164). The expression levels of these four genes in antennae were reduced four- to ninefold (Fig. 4c). Mosquitoes injected with dsRNA of GFP were also prepared as controls. Both sexes with *Orco* or *LOR* knockdown lost preference to longifolene, with no difference among the non-injected mosquitoes and those injected with dsGFP (dsRNA for GFP), dsPOR1 (dsrRNA for POR1) or dsPOR2 (dsRNA for POR2) ($P > 0.05$, one-way ANOVA with Tukey's multiple-comparison test, $n = 6$) (Fig. 4d). Moreover, mosquitoes with *Orco* or *LOR* knockdown lost preference to *M. robertsii*-colonized *G. mellonella* cadavers, with no difference between non-injected and dsGFP-injected mosquitoes ($P > 0.05$, one-way ANOVA with Tukey's multiple-comparison test, $n = 6$) (Fig. 4e). EAG assays showed that both sexes of adult mosquitoes injected with dsGFP showed robust responses to longifolene in a dose-dependent manner (Fig. 4f,g). At each dosage, responses of dsGFP-injected mosquitoes were 3–15-fold greater than those injected with dsOrco (dsRNA for Orco) or dsLOR (dsRNA for LOR) ($P < 0.001$, one-way ANOVA with Tukey's multiple-comparison test, $n = 10$); no difference was found between dsLOR- and dsOrco-injected males ($P > 0.05$), while the response of dsLOR-injected females was slightly but significantly greater than that of dsOrco-injected females ($P < 0.05$) (Fig. 4f,g).

Construction of *Metarhizium* strains producing mosquito-attractive cultures on media

As insects are not suitable substrates for massive production of mosquito-attracting spores for mosquito control, we sought to develop *Metarhizium* strains whose spores, preferably produced in the cheap BRH (wheat bran, rice and rice husk) medium to allow cost-effective mass production, can emit longifolene to attract mosquitoes for higher infection rates and control efficacy. To this end, we used *M. robertsii*, a model in transgenic studies with weak virulence against mosquitoes[16], and an *M. pingshaense* strain (Extended Data Fig. 5a), which has a strong mosquito-killing capability (see below). The 12-day *M. pingshaense*-colonized *G. mellonella* cadavers differed from those colonized by *M. robertsii* in VOC types and longifolene (0.056 ng g^{-1} cadaver per h) (Supplementary Fig. 3b) produced at 2-fold lower levels (Fig. 2c) ($P < 0.01$, two-tailed Student's *t*-test). *M. robertsii*-colonized cadavers were thus more attractive to *D. melanogaster* larvae than *M. pingshaense*-colonized cadavers (74.4% versus 25.6%) ($P < 0.01$, two-tailed Mann–Whitney test) (Supplementary Fig. 3e). *M. pingshaense* also produced different VOCs from *M. robertsii* when grown on BRH medium with longifolene not detected in *M. pingshaense*, but in *M. robertsii* (Supplementary Fig. 4); the most abundant volatile produced by *M. pingshaense* was thujopsene (31.7%) followed by 1-octen-3-ol (28.7%) (Fig. 5a).

We further tried to construct transgenic *Metarhizium* strains, cultures of which, when produced on BRH medium, can emit sufficient longifolene to attract mosquitoes. Expression of the pine (*Pinus sylvestris*) longifolene synthase TPS (ABV44454) enabled the *Saccharomyces cerevisiae* yeast to produce longifolene[17], which was thus expressed in *M. robertsii* and *M. pingshaense* to produce Mr-*Tps* (Extended Data Fig. 6a) and Mp-*Tps* (Fig. 5b), respectively. Mr-*Tps* and Mp-*Tps* closely resembled their parental species in pathogenicity, spore yield and lipid droplet formation (Extended Data Figs. 6 and 7). Thus, an average of one spore (Mp-*Tps* or the WT) per mosquito caused ~50% mortality (Extended Data Fig. 7c). Similar to the WT[16], Mr-*Tps* also showed weak virulence against mosquitoes (Extended Data Fig. 6e).

Fig. 3 | *M. robertsii*-colonized *G. mellonella* cadavers emit longifolene that attracts *D. melanogaster* by activating its olfactory system. a, Two-way choice assays of the WT larvae response to increasing longifolene doses (versus hexane, used for preparation of longifolene solutions, which is applicable for all similar assays). The box plots show the median (centre line), the interquartile range (box bounds, 25th to 75th percentiles), and the minima and maxima within 1.5× interquartile range from the box (whiskers) (used for the response index in **b**, **e**, **h** and **i** of this figure). Values with different larvae are significantly different ($P < 0.05$, one-way ANOVA with Tukey's multiple-comparison test, $n = 9$). **b**, Two-way choice assays of larval response to longifolene (10^{-5} g): WT; mutant *Orco*^{2}, *Or43b*^{l4}, *Or43b*$^{1.w-}$ and *Or74a*^{D31}; Or43b and Or74a-deficient lines (Or-GAL4/UAS-TNT system); and controls. Values with different larvae are significantly different ($P < 0.01$, one-way ANOVA with Tukey's multiple-comparison test, $n = 10$). Other deficiency line data are shown in Extended Data Fig. 2. **c**, SSR showing T1 ORNs expressing Or43b (*UAS-Or43b;Or67d*^{GAL4} (genotype: *w; UAS-Or43b; Or67d*^{GAL4})) or Or74a (*UAS-Or74a;Or67d*^{GAL4} (genotype: *w; UAS-Or74a; Or67d*^{GAL4})) respond to longifolene dose-dependently. Parental controls: *Or67d*^{GAL4} (genotype: *w; Sp/CyO; Or67d*^{GAL4}), *UAS-Or43b* (genotype: *w; UAS-Or43b;+*) and *UAS-Or74a* (genotype: *w; UAS-Or74a;+*). Hex, blank control hexane. Data are presented as mean ± s.e. Values with different red or blue letters indicate significant differences among dosages for *UAS-Or43b;Or67d*^{GAL4} (*UAS-Or74a;Or67d*^{GAL4}) ($P < 0.05$, Kruskal–Wallis test followed by Dunn's multiple-comparison test, $n = 10$). The asterisks indicate significant differences between lines at each dose (***$P < 0.001$, two-tailed Student's *t*-test). NS, no significant difference among lines for the blank control ($P > 0.05$, two-tailed Student's *t*-test). **d**, Representative SSR response traces (of ten independent experiments) of *Or67d*^{GAL4}, *UAS-Or43b* and *UAS-Or43b;Or67d*^{GAL4} (left), and the lines *Or67d*^{GAL4}, *UAS-Or74a* and *UAS-Or74a;Or67d*^{GAL4} (right). **e**, Contribution of longifolene to the attractiveness of 12-day *M. robertsii*-colonized *G. mellonella* cadavers to *D. melanogaster* larvae. Left panel: two-way choice assay of WT, *Orco*^{2}, *Or74a*^{D31}, *Or43b*^{l4} and *Or43b*$^{1.w-}$ larvae response to the mycosed cadavers versus freeze-killed healthy *G. mellonella* larvae. Right panel: *M. robertsii* infection-caused mortalities of larvae 4 days after 10 min of exposure to the mycosed cadavers. Values with different letters are significantly different ($P < 0.05$, one-way ANOVA with Tukey's multiple-comparison test for all comparisons, $n = 10$). **f**, GC–EAD analysis of longifolene (10^{-7} g)-elicited antennal response of both sexes of the WT *D. melanogaster* and *A. albopictus* adults. Images are representative of ten independent experiments. **g**, EAG assays of dose antennal response to longifolene: WT, *Orco*^{2}, *Or74a* and *Or43b* mutant adults. Values shown: treatment minus control (hexane). Data are presented as mean ± s.e. At each dose, values with different letters are significantly different ($P < 0.05$, one-way ANOVA with Tukey's multiple-comparison test, $n = 10$). **h**,**i**, Two-way choice assays of WT, *Orco*^{2}, *Or74a* and *Or43b* mutant male and female adult responses to longifolene (10^{-4} g) (versus hexane) (**h**) and the mycosed cadavers (versus freeze-killed healthy *G. mellonella* larvae) (**i**). Values with different letters are significantly different ($P < 0.05$, one-way ANOVA with Tukey's multiple-comparison test). *n*, experiment repeats.

Similar to Mr-*Tps* (Extended Data Fig. 6f and Supplementary Results), Mp-*Tps* produced 205-fold more longifolene (24.1 ng g^{-1} cadaver per h) than the WT on *G. mellonella* cadavers (Supplementary Fig. 3b). Unlike the WT, Mp-*Tps* produced longifolene in BRH (97.6 ng g^{-1} BRH culture per h) (Fig. 5a) and PDA (210.3 ng g^{-1} PDA mycelium per h) (Supplementary Fig. 4a). Mp-*Tps* cultured on BRH (designated as Mp-*Tps* BRH cultures) did not differ from the WT in 1-octen-3-ol production ($P > 0.05$, two-tailed Student's *t*-test, $n = 3$)

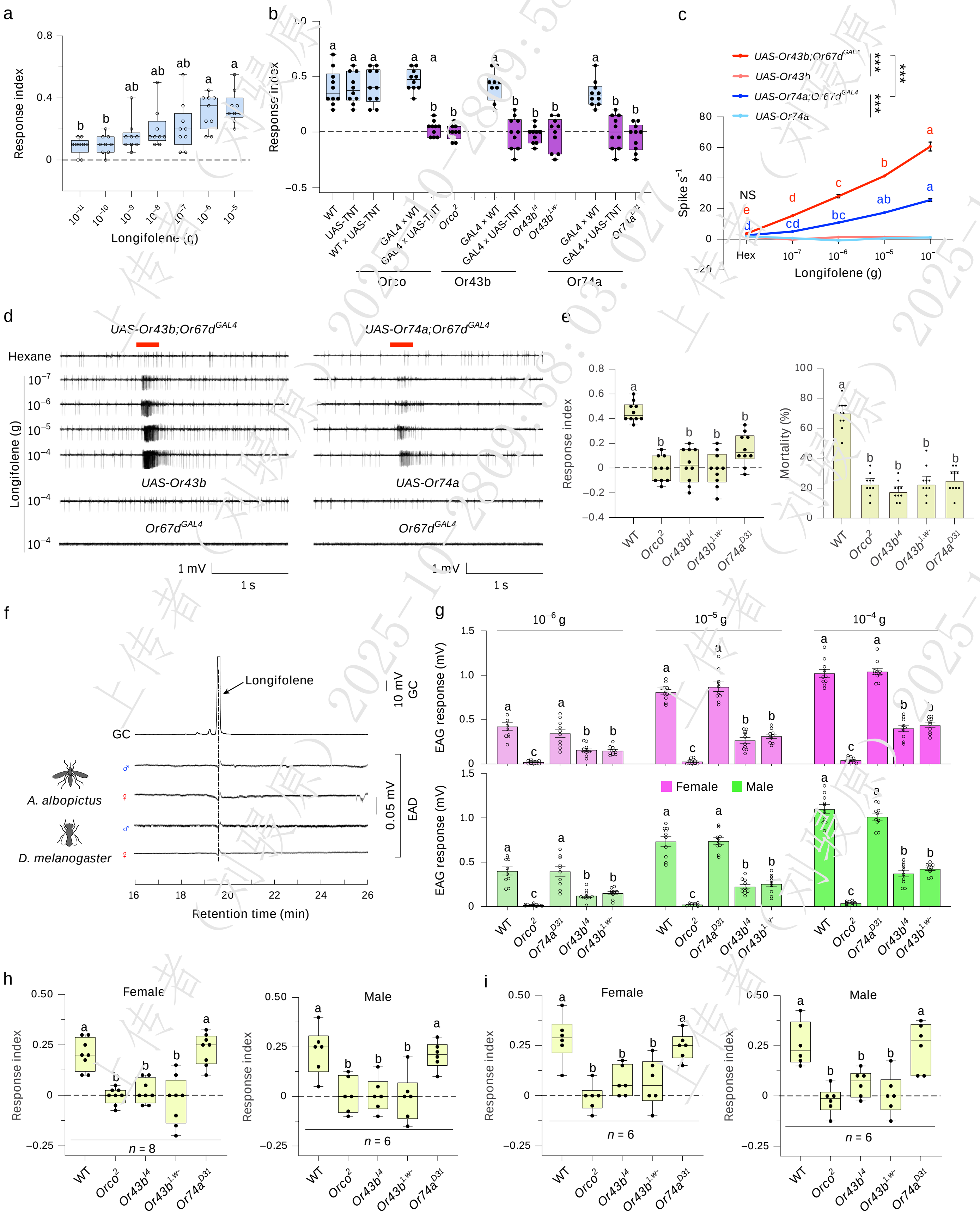

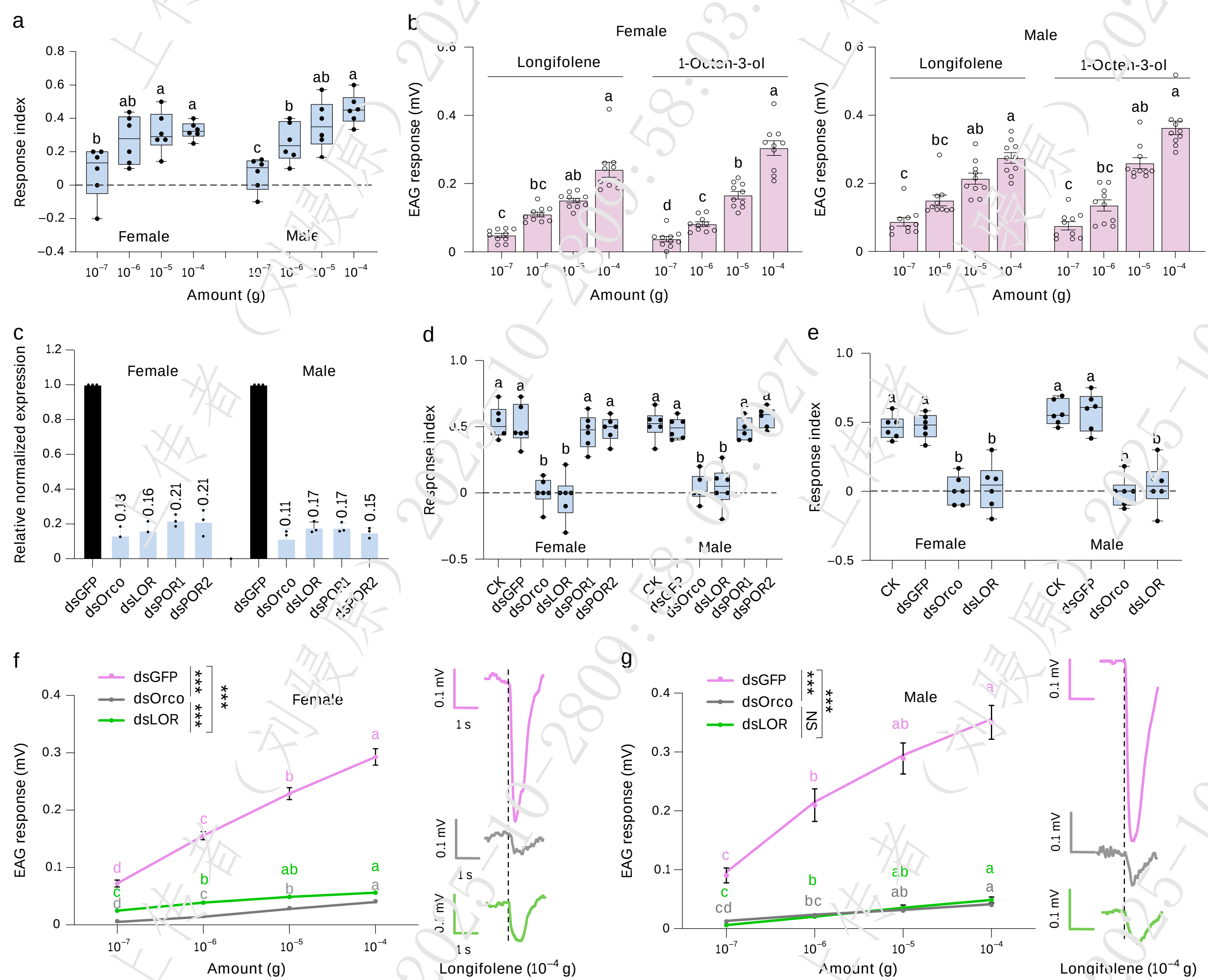

Fig. 4 | Longifolene is attractive to mosquitoes. a, Two-port olfactometer assays of the behavioural response of male and female *A. albopictus* adults to increasing longifolene doses (versus hexane). The box plots show the median (centre line), the interquartile range (box bounds, 25th to 75th percentiles), and the minima and maxima within 1.5× interquartile range from the box (whiskers) (used for the response index in **d** and **e** of this figure). Within each gender, values with different letters are significantly different ($P < 0.05$, one-way ANOVA with Tukey's multiple-comparison test, $n = 6$). **b**, EAG assays of dose antennal response to longifolene and 1-octen-3-ol (positive control). Values were calculated by subtracting the control (hexane) from each treatment. For each sex, values with different letters are significantly different within a VOC ($P < 0.05$, one-way ANOVA with Tukey's multiple-comparison test, $n = 10$). **c**, qRT-PCR analysis of *Orco*, *LOR*, *POR1* and *POR2* expression in antennae of mosquitoes injected with their respective dsRNA. The analysis was repeated three times. Values represent fold changes of gene expression compared with dsGFP injection, which is set to 1. Data are presented as mean ± s.e. **d**, Two-port olfactometer assays of behavioural response to longifolene (10^{-4} g) of both sexes of non-injected (CK) mosquitoes, and mosquitoes injected with dsGFP, dsOrco, dsLOR, dsPOR1 or dsPOR2. Values with different letters are significantly different ($P < 0.05$, one-way ANOVA with Tukey's multiple-comparison test, $n = 6$). **e**, Two-port olfactometer assays of response to 12-day *M. robertsii*-colonized *G. mellonella* cadavers (versus freeze-killed healthy *G. mellonella* larvae) of both sexes of non-injected mosquitoes, and mosquitoes injected with dsGFP, dsOrco or dsLOR. Values with different letters are significantly different ($P < 0.05$, one-way ANOVA with Tukey's multiple-comparison test, $n = 6$). **f**,**g**, EAG assays of dose antennal response to longifolene of female (**f**) and male (**g**) mosquitoes injected with dsGFP, dsOrco or dsLOR. The EAG traces represent antennal response to 10^{-4} g of longifolene; traces are representative of 10 independent experiments. For each mosquito line, values with different letters are significantly different among dosages ($P < 0.001$, one-way ANOVA with Tukey's multiple-comparison test, $n = 10$). Asterisks indicate significant differences among different mosquito lines at each dose (***$P < 0.001$, two-tailed Student's t-test). NS, no significant difference among different lines ($P > 0.05$, two-tailed Student's t-test). Data presented as mean ± s.e.

(Fig. 5a). Mp-*Tps* and the WT BRH cultures were both attractive to *A. albopictus* mosquitoes of either sex, but Mp-*Tps* BRH cultures were more attractive than the WT to females (62.3% versus 37.7%) and males (70.6% versus 29.4%) ($P \leq 0.02$, two-tailed Mann–Whitney test, $n = 7$) (Fig. 5c), presumably due to them simultaneously emitting longifolene and 1-octen-3-ol (Fig. 5a). Whereas longifolene emission was detected from a pile of 50 Mp-*Tps*-colonized *A. albopictus* cadavers, single cadavers did not produce detectable levels and were not insect attractive, probably owing to minuscule fungal biomass (1.4×10^6 spores per cadaver) (Extended Data Fig. 7f–h).

Mp-*Tps* BRH cultures efficiently attract and kill mosquitoes

We then assayed the control efficacy of Mp-*Tps* BRH cultures against *A. albopictus* mosquitoes. Adult mosquitoes were released in 1-m³ cages

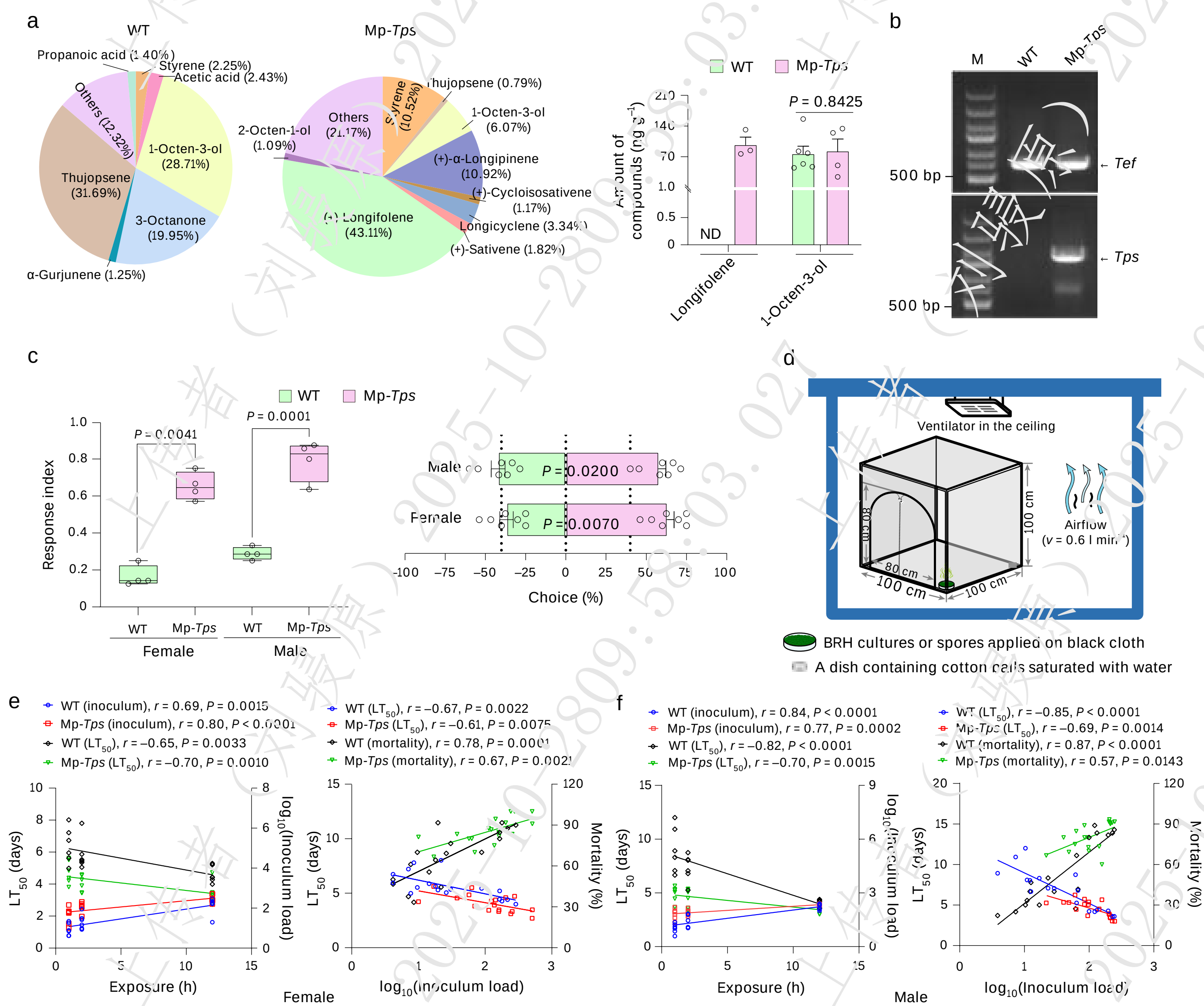

Fig. 5 | Construction of the transgenic strain Mp-*Tps* that can attract and kill laboratory-reared adult *A. albopictus* mosquitoes. a, Percentages of major VOCs released by BRH cultures of the WT (the parental WT strain of Mp-*Tps*) (left) and Mp-*Tps* (middle), and actual amount of longifolene and 1-octen-3-ol produced (right). In the left and middle panels: percentage contribution of each VOC to the total VOC production (based on peak area) in parentheses; representative of five assays. In the right panel: ND, not detectable. Two-tailed Student's *t*-test was used ($n = 5$). Data are presented as mean values ± s.e. **b**, RT-PCR confirmation of the expression of the pine longifolene synthase gene *Tps* in Mp-*Tps*. M, DNA ladder; *Tef*, reference gene encoding the translation elongation factor. Images are representative of three independent experiments. **c**, Two-port olfactometer assays of mosquito behavioural preference. Left panel: BRH medium versus Mp-*Tps* or the WT BRH cultures. The box plots show the median (centre line), the interquartile range (box bounds, 25th to 75th percentiles), and the minima and maxima within 1.5× interquartile range from the box (whiskers). Right panel: Mp-*Tps* versus the WT BRH cultures. Data are presented as mean ± s.e. Two-tailed Mann–Whitney test was used ($n = 4$ (left) and 7 (right)). **d**, Schematic diagram of the experimental setup to inoculate mosquitoes in 1-m^3 cages with spores on black cloth (1.4×10^5 spores per cm^2) or sporulated BRH cultures (10 g in a 9-cm Petri dish). **e**,**f**, Females (**e**) and males (**f**): correlations between exposure duration to fungal BRH cultures and LT_{50} values or inoculum load per mosquito (log transformation) (left) and between inoculum load and LT_{50} values or mortality (right). Calculations were conducted with two-tailed Pearson's correlation.

and exposed for 1 h, 2 h or 12 h to BRH cultures placed on the bottom side (Fig. 5d). After a 1-h exposure, more mosquitoes of both sexes were contaminated with Mp-*Tps* spores than the WT (Extended Data Fig. 8), and males picked up more Mp-*Tps* spores than females ($P < 0.001$, two-tailed Mann–Whitney test) (Extended Data Fig. 9a). To determine why this happened, we assayed mosquito visitation to fungal BRH cultures within a 1-h exposure. Males and females visited Mp-*Tps* 3.1- and 2.7-fold more frequently, respectively, than the WT, and the cumulative time males and females spent on Mp-*Tps* was 12.6- and 5.4-fold longer, respectively, than the WT ($P < 0.05$, two-tailed Student's *t*-test) (Extended Data Fig. 9c). Males visited Mp-*Tps* 2.1-fold more frequently than females, and the cumulative time males spent on the cultures was 2.4-fold longer than the females ($P < 0.05$, two-tailed Student's *t*-test) (Extended Data Fig. 9c and Supplementary Videos 3 and 4). For both sexes, inoculum load (the number of spores per mosquito) positively correlated with the number of visits to Mp-*Tps* and the cumulative time spent on the cultures (Extended Data Fig. 9d). Both Mp-*Tps* and the WT achieved 100% inoculation rates with 2 h or more of exposure (Extended Data Fig. 8). Inoculum load increased with exposure time ($r \geq 0.69$, $P < 0.01$) and negatively correlated with LT_{50} values (median lethal time) ($r \leq -0.65$, $P < 0.05$) (Fig. 5e,f). Regardless of the exposure time, mosquitoes picked up more Mp-*Tps* spores than the WT, and

 https://doi.org/10.1038/s41564-025-02155-9

Mp-*Tps* killed both sexes approximately 1.4-fold faster than the WT ($P < 0.05$, two-tailed Student's *t*-test) (Extended Data Fig. 8).

In addition to *A. albopictus*, Mp-*Tps* was also more effective than the WT against *A. sinensis* and *Culex pipiens* mosquitoes. Longifolene emission and mosquito attraction and the killing capability of Mp-*Tps* BRH cultures can last 8 weeks (Supplementary Results).

Testing attraction of wild-caught mosquitoes in a room with human and plant odours

We examined the effectiveness of Mp-*Tps* BRH cultures in attracting and killing wild-caught mosquitoes in a large room (6.5 m (length) × 5.5 m (width) × 3 m (height)) (Fig. 6a). As the efficacy of spore-borne attractiveness may be compromised by environmental mosquito attractants, we studied the impact of humans (hosts) and mosquito-attracting flowering plants (sugar sources) on the ability of Mp-*Tps* to attract and kill mosquitoes.

Wild-caught *A. albopictus* larvae were collected and reared in the laboratory to obtain adults (Fig. 6b and Extended Data Fig. 5b). Similar to laboratory-reared mosquitoes, Mp-*Tps* were more attractive than the WT to wild-caught females (73.1% versus 26.9%) and males (81% versus 19%) ($P < 0.0001$, two-tailed Student's *t*-test, $n = 6$) (Fig. 6c). We then compared the ability of the WT and Mp-*Tps* to attract and kill mosquitoes in the large room with volunteers sleeping under mosquito netting in the centre of the room. To maximize host searching, tests were conducted with 7- to 12-day-old mated mosquitoes that had never had a blood meal. Overnight (~12 h) exposure led to ~71% of both sexes being contaminated with the WT spores compared with 100% with Mp-*Tps* (Fig. 6d), with Mp-*Tps* inoculum loads approximately 10-fold greater ($P < 0.0001$, two-tailed Mann–Whitney test) (Fig. 6d).

Strong negative correlations ($r \le -0.88$, $P < 0.0001$) were found between inoculum load and LT_{50}, and positive correlations between inoculum load and mortality ($r \ge 0.8$, $P \le 0.002$) (Fig. 6d). Thus, without a human subject, Mp-*Tps* killed females and males 2.2- and 2.3-fold faster, respectively, than the WT ($P < 0.05$, two-tailed Student's *t*-test) (Fig. 6d). Mp-*Tps* caused 100% mortality in males and females at ~10 days and 13 days post-exposure, respectively, while the WT exposure had killed 57% females and 86% males by the experimental end point (15 days post-exposure) (Extended Data Fig. 10a). Human presence had no significant effects on these parameters for either Mp-*Tps* or the WT ($P > 0.05$, two-tailed Student's *t*-test) (Fig. 6d), and no significant difference in the WT inoculum load or killing speed was found between the sexes ($P > 0.05$). However, irrespective of human presence, males picked up more Mp-*Tps* spores than females and died significantly faster ($P < 0.05$, two-tailed Student's *t*-test) (Fig. 6d).

Nectar-rich flowering Mexican petunias (*Ruellia brittoniana*) were attractive to both sexes of *A. albopictus* adults (Extended Data Fig. 10b and Supplementary Results). They were placed in the centre of the large room with sugar-starved or sugar-fed mosquitoes. Irrespective of the mosquito nutrient status and sex, plants reduced the inoculum loads of Mp-*Tps* and the WT >4-fold ($P < 0.05$, two-tailed Mann–Whitney test) (Fig. 6e). Negative correlations were found between the inoculum load and LT_{50} ($r < -0.69$, $P \le 0.001$) (Fig. 6f). Males thus lived 1.5- to 2.4-fold longer with plants present (Fig. 6e). By the experimental end point, Mp-*Tps* still caused 93% and 100% mortality in fed and starved males, respectively, which were significantly greater than those of the WT (64% of fed and 79% of starved) ($P < 0.05$, two-tailed Student's *t*-test) (Fig. 6e and Extended Data Fig. 10c,d). Females were less impacted by plants as a slight reduction in the rate Mp-*Tps* killed starved and fed females was not significant ($P > 0.05$, two-tailed Student's *t*-test) (Fig. 6e). Even with plants, Mp-*Tps* caused 91% and 95% mortality in fed and starved females, respectively, which were significantly greater than those of the WT (57% of fed and 70% of starved) ($P < 0.05$, two-tailed Student's *t*-test) (Fig. 6 and Extended Data Fig. 10c,d).

Discussion

Entomopathogenic fungi are the most common insect pathogens and major regulators of insect populations[18]. Their efficacy depends on effective spore dispersal. To facilitate dispersal, many narrow-host-range fungi hijack the behaviour of living hosts so that spores are produced at a time and place where hosts are present. This process requires specific evolution to an individual host species reducing the possibility of host jumps[19,20]. Broad-host-range pathogens were assumed to linger in the environment waiting for wind, rain or passing animals for dispersal, and coming across their hosts by chance. However, here we show that *M. robertsii*, a keystone organism in ecosystems[21], disperses spores from exploited cadavers using broad-spectrum insect attractants to lure new hosts, confirming that manipulating arthropod behaviour is not unique to specialists. Both spore dispersal strategies (altering the behaviour of infected insects or producing attractant-emitting spores on dead insects) increase fungal fitness.

Metarhizium infect diverse hosts via penetration of the cuticle or foregut, are eaten and discharged in faeces to infect fresh hosts, or develop symbiosis with plant roots[22]. *M. robertsii*-colonized insect cadavers release longifolene and geosmin. While geosmin attracts some insects, including mosquitoes, it repels others such as *D. melanogaster*[23,24]. Longifolene is the major contributor to attraction facilitating infection. Or43b is involved in the response of adult *D. melanogaster* to longifolene and the cadavers, while Or43b and Or74a, which respond to multiple fruit volatiles[25], need simultaneous activation for larvae to respond. Similarly, co-activation of two specific receptors is required for pyrethrum to alter fly behaviour[26]. Although Or43b is known to be expressed in larvae[27], it has only been documented to have functions in adults[28]. In this study, two lines of evidence confirmed that Or43b also functions in larvae. First, larvae of two different Or43b mutants did not respond to longifolene and the cadavers. Second, *Or43b* is expressed in larvae. Homologues of *Drosophila* longifolene receptors are found in many insect species, and we determined that the Or43b homologue LOR is the longifolene receptor in *A. albopictus*. This could explain why *Metarhizium*-colonized insect cadavers attract a wide range of insects with different food preferences.

Fig. 6 | The ability of fungal BRH cultures to attract and kill wild-caught *A. albopictus* mosquitoes in a large space with and without competition from human or plant odours. **a**, Schematic diagram illustrating the large room used in this study. The human and the bed are approximately scaled to the room dimension. **b**, *A. albopictus* adults for this study were reared from larvae obtained using oviposition traps (black buckets with hay immersed in water). Morphological characteristics were used to distinguish male and female *A. albopictus* adults. Images are representative of at least ten independent experiments. **c**, Two-port olfactometer assays of mosquito behavioural preferences to Mp-*Tps* and the WT (the parental WT strain of Mp-*Tps*) BRH cultures. Data are presented as mean ± s.e. Two-tailed Student's *t*-test was used ($n = 6$). **d**, Impacts of human odours. Left panel: inoculum load (horizontal line: medians, also used in **e** in this figure) and inoculation rate. Middle panel: LT_{50} values (data are presented as mean ± s.e., also used in **e** in this figure) and mortality at 15 days post-exposure. Right panel: correlations between inoculum load per mosquito (log transformation) and LT_{50} value (two-tailed Pearson's correlation, also used in **f** in this figure) and mortality (two-tailed Spearman's rank correlation, also used in **f** in this figure). *R*, experiment repeats; *n*, total number of mosquitoes assayed. For the inoculum load and LT_{50} values, two-tailed Student's *t*-test was used for normally distributed data and two-tailed Mann–Whitney test was used for non-normal data (also used in **e** in this figure). Values with different letters in the inoculation rate or mortalities of the WT and Mp-*Tps* are significantly different (two-tailed Student's *t*-test, *P* values given below) (also used in **e** in this figure). **e**, Impacts of flowering plants on sugar-fed and sugar-starved mosquitoes. Upper panel, inoculum load and inoculation rate; lower panel, LT_{50} values and mortality at day 15 post-exposure. **f**, Correlations between inoculum load and LT_{50} value and mortality presented in **e**.

The transgenic strain Mp-*Tps* attracted both sexes of adult mosquitoes, implying that attraction was not related to female-specific oviposition site selection or host seeking. We confirmed this by showing that human presence did not effectively compete with the attractiveness of Mp-*Tps* to male and female mosquitoes. Plants are the dominant mosquito sugar sources and the only food source for males[29]. The presence of mosquito-attracting Mexican petunia compromised the attractiveness of Mp-*Tps*, suggesting that longifolene-emitting Mp-*Tps*

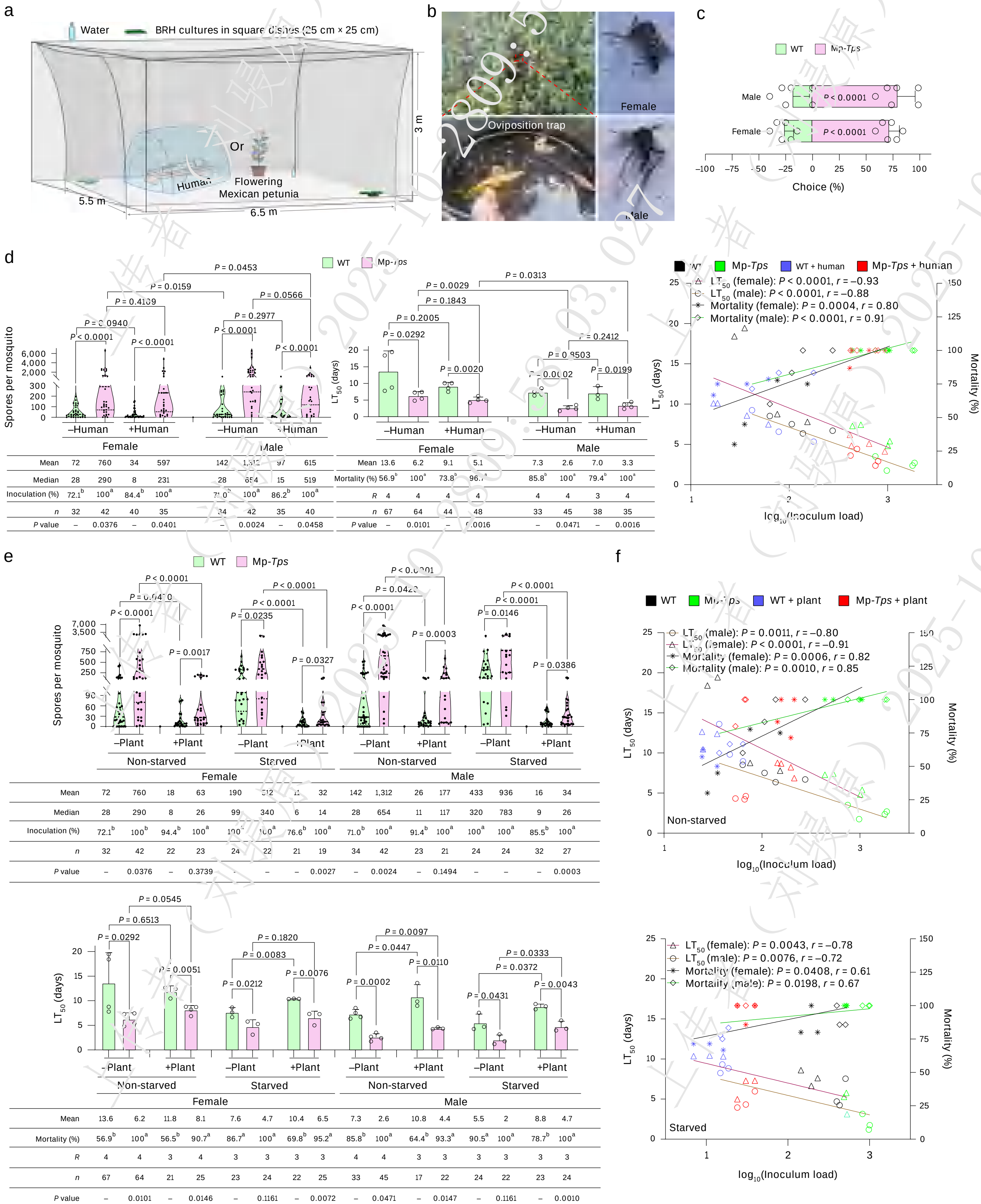

BRH cultures mimic plant sugar sources. However, even in an indoor area approximately 12-fold larger than western African experimental huts recommended by the World Health Organization (WHO)[30], Mp-*Tps* infection caused approximately 91% mortality by competition with Mexican petunia, which exceeded the WHO 80% control threshold for a successful agent[31].

Mp-*Tps*-infected mosquitoes probably die in the environment and develop into sporulated mycelium-covered cadavers. The chances of the cadavers causing negative ecological impacts are low for several reasons. First, like previously reported *M. pingshaense* strains[3,4,32,33], our strain could also have host preference retained in Mp-*Tps*. Although assays with more insect species are needed to determine the host preference of Mp-*Tps*, this study showed that it preferred mosquitoes over *G. mellonella* as approximately 12,500-fold more spores were needed to achieve similar lethality in *G. mellonella* to that in mosquitoes (Extended Data Fig. 7). Secondly, mosquitoes are solitary, suggesting that Mp-*Tps*-colonized mosquito cadavers will exist individually; the minuscule mycelia on single cadavers emitted trace longifolene unable to attract mosquitoes even in small assay devices, let alone in environments where plant-derived longifolene is common[34]. It is likely that ants feed on Mp-*Tps*-killed mosquitoes, but ant colonies are resistant to *Metarhizium* because of social behavioural immunity[35]. Moreover, Mp-*Tps* spores on mosquito cadavers could gradually die off like spores on *M. robertsii*-colonized *G. mellonella* cadavers, further reducing the chance for other insects to be contaminated by sufficient active Mp-*Tps* spores for infection from mosquito cadavers. Thirdly, although some *M. pingshaense* strains were reported to be beneficial plant root symbionts, a previous study with two *M. pingshaense* strains showed that their plant-associated populations were small[32], so chances are low that Mp-*Tps* spores on single mosquito cadavers build up sufficient plant-associated populations for attracting insects for infection. Similarly, it is unlikely that the miniscule Mp-*Tps* mycelia on single mosquito cadavers could outcompete fast-growing fungi such as *Aspergillus* to build up a sufficient biomass for attracting insects on accidentally available nutrient-rich substrates. Finally, longifolene is safe for humans, animals, plants and microorganisms[36–40]. Nevertheless, to determine the ecological impacts of Mp-*Tps*, field trials are needed to evaluate its environmental persistence and impacts on non-target insects. Mp-*Tps* could be further optimized to mitigate potential ecological impacts. For example, CRISPR–Cas9-mediated gene insertion without usage of foreign selection markers could be developed to construct a new version of Mp-*Tps* with the *Tps* gene inserted into the known genes involved in UV resistance or plant colonization[41,42], thereby disrupting this gene and reducing environmental persistence.

Limitation of this study

We showed that the transgenic strain Mp-*Tps* efficiently controlled wild-caught mosquitoes in a large room with humans or mosquito-attracting plants. However, real mosquito environments are more complex, rendering laboratory simulations inadequate. Consequentially, a limitation of our research is that the mosquito control efficacy of Mp-*Tps* has not been determined in authentic environmental conditions. In future, field trials will be necessary to comprehensively assess its mosquito control efficacy and inform further research for developing efficient and safe Mp-*Tps*-based mosquito control agents.

Methods

Fungal and bacterial strains

Escherichia coli DH5α cells were used to construct plasmids. Fungal transformations were mediated by *Agrobacterium tumefaciens* AGL1 (ref. 43).

M. robertsii (ARSEF2575) was obtained from the Agricultural Research Service Collection of Entomopathogenic Fungi (ARSEF) in Ithaca, New York. The GFP-labelled *M. robertsii* strain GFP-WT was previously constructed[44].

M. pingshaense TM1 was isolated in grassland soil in the Tianmu Mountains, Hangzhou, China (this study). Taxonomic identification of this isolate was conducted by phylogenetic analysis of the DNA sequence encoding the 5′ end of elongation factor 1-α (5′TEF)[45]. Following cloning by PCR, the 5′TEF in the isolated *Metarhizium* strain was combined with 18 taxonomically authenticated 5′TEF reference sequences representing 9 *Metarhizium* species (Extended Data Fig. 5a). All PCR primers used in this study are shown in Supplementary Table 2. High-fidelity Taq DNA polymerase (KOD Plus Neo) was used for all PCRs, and all PCR products were confirmed by DNA sequencing. Phylogenetic identification of the isolate was inferred under a GTRGAMMA model by maximum likelihood and neighbour-joining phylogenetic reconstruction with MEGA 7.0 (ref. 46). A Bayesian inference tree was constructed using MrBayes v3.2.5 as described[47].

Insects and plants

Mexican petunia plants (*R. brittoniana*) were purchased from local markets and maintained in the laboratory at room temperature.

G. mellonella larvae (last instar) were purchased from Ruiqing Bait. The adult whitefly *B. tabaci* and cotton mealybug *P. solenopsis* were gifts from X. Wang and M. Jiang, respectively, at the Institute of Insect Sciences at Zhejiang University. *L. boulardi* wasps were also maintained at the Institute of Insect Sciences at Zhejiang University. *A. albopictus* mosquitoes were maintained at the Institute of Microbiology at Zhejiang University. *A. sinensis* and *C. pipiens* mosquitoes were reared in the insectarium of Jiangsu Institute of Parasitic Diseases.

All *D. melanogaster* stocks were maintained on standard cornmeal–molasses–agar medium at 25 °C in 6-ounce, square-bottom plastic fly bottles[48]. All experiments with WT *D. melanogaster* were performed using the Canton-S. The Or-GAL4 lines[27,49] were obtained from the Bloomington Drosophila Stock Centre, including *Or7a-GAL4* (BL#23908), *Or10a-GAL4* (BL#9944), *Or13a-GAL4* (BL#9945), *Or19a-GAL4* (BL#23887), *Or30a-GAL4* (BL#9960), *Or33a-GAL4* (BL#9962), *Or33b-GAL4* (BL#9964), *Or35a-GAL4* (BL#9967), *Or42a-GAL4* (BL#9970), *Or42b-GAL4* (BL#9971), *Or43b-GAL4* (BL#23894), *Or45a-GAL4* (BL#9976), *Or45b-GAL4* (BL#9977), *Or49a-GAL4* (BL#9985), *Or59a-GAL4* (BL#9989), *Or63a-GAL4* (BL#9992), *Or67b-GAL4* (BL#9996), *Or74a-GAL4* (BL#23124), *Or85c-GAL4* (BL#23914), *Or88a-GAL4* (BL#23137), *Or94b-GAL4* (BL#23916) and *Orco-GAL4* (BL#23292). The other *D. melanogaster* lines used were *Orco^{1}* (BL#23130), *UAS-mCD8-RFP* (BL27399), *UAS-TNT* (BL#28838), the *Or43b* mutant *Or43b$^{1.w-}$* (BL#97369) and the line with the attP docking site on the second chromosome (BDSC_25709).

The involvement of the 21 larval ORs in larval response to longifolene and hexane (control) was assayed using the Or-GAL4–UAS-TNT system[13]. To this end, each Or-GAL4 line was crossed with the UAS-TNT line to block synaptic transmission of ORNs.

From August to October 2023, we used oviposition traps (black buckets with hay immersed in water) to collect wild *A. albopictus* larvae in Jiangsu Institute of Parasitic Diseases (Fig. 6b). Larvae were collected from the traps every 2 weeks and reared in the laboratory to allow pupation and adult emergence. We confirmed *A. albopictus* identity through morphological characteristics of adults (Fig. 6b) and phylogenetic analysis using the mitochondrial COI (*Mt-COI*) gene. Total DNA was extracted from adults and the *Mt-COI* gene PCR cloned. Sequences from three randomly selected females and males were combined with eight taxonomically authenticated *Mt-COI* sequences representing *Aedes* species (Extended Data Fig. 5b). Phylogenetic analysis was conducted as described above for identification of *M. pingshaense* strain TM1.

Analysis of *D. melanogaster* behavioural preferences using two-choice assays

Two-choice assays of the attractiveness to *D. melanogaster* larvae of longifolene, isolongifolene, *Metarhizium*-colonized *G. mellonella* larval cadavers, *Metarhizium* BRH cultures and *Metarhizium* mycelia separated from insect cadavers and media, and lipid droplets were modified from a previous study[50]. To assay longifolene or isolongifolene, they were dissolved in hexane and applied to three layers of white filter paper (diameter = 0.5 cm), with hexane alone as control. For lipid droplets, 10 µl of lipid droplets was also applied to three layers of filter paper with 10 µl 2-[4-(2-hydroxyethyl)piperazin-1-yl] ethane-1-sulfonic acid (HEPES) buffer (used for preparation of lipid droplets (see below)) as controls. Controls for *Metarhizium*-colonized *G. mellonella* larval cadavers, *Metarhizium* BRH cultures, and mycelia from cadavers or media were freeze-killed healthy *G. mellonella* larvae (uninfected control cadavers), BRH medium and water-soaked cotton balls, respectively (Supplementary Table 3). Assays were conducted in 9-cm Petri dishes containing 2% water agar. A stimulus and its control were placed on opposite sides of the Petri dishes. Approximately 20 3rd instar larvae were placed in the centre (release point) of a Petri dish that was divided into 4 zones: 2 'no choice' zones, 1 preferred zone containing the stimulus and 1 non-preferred zone containing the control (Supplementary Fig. 5a). After 10 min at 26 °C, larvae in each zone were counted. The response index, showing stimulus attractiveness, was calculated as $(O-C)/T$, where O was the number of larvae in the preferred zone, C was the number in the non-preferred control zone and T was the total number of larvae assayed. A stimulus was considered to be attractive when the response index exceeded zero. When comparing 2 stimuli (1 and 2), they were placed on opposite sides of 9-cm Petri dishes, also divided into 4 zones: 2 'no choice' zones, stimulus 1 zone and stimulus 2 zone. Approximately 20 3rd instar larvae were placed at the release point, and after 10 min, larvae in the stimulus 1 zone and stimulus 2 zone were counted to calculate behavioural preference as described[51]. Briefly, behavioural preference was shown as the percentage of insects in either stimulus zone out of the total of insects that had made a choice, which was calculated as N1 or N2/(N1 + N2), where N1 was the number of insects in the stimulus 1 zone and N2 was the number in the stimulus 2 zone. The calculations for response index (stimulus versus its control) and behavioural preference (two stimuli were compared) are applied in all similar two-way choice assays and two-port olfactometer assays in this study. All behavioural assays in the study were repeated at least four times and summarized in Supplementary Table 3.

The behavioural preference of *D. melanogaster* adults was assayed using a two-choice trap experiment[52]. Briefly, assays were conducted in transparent plastic boxes (12 × 8 × 10 cm), with 10 holes (diameter = 1 mm) for aeration and wet cotton balls (in two 3-cm Petri dishes at opposite corners) as water source. Glass vials (10 ml) were used as traps with 1-ml pipette tips (tip mouth cut to a diameter of 2.5 mm) inserted into the vial lids to allow the flies to enter (Supplementary Fig. 5b). Two traps (one for a stimulus, one for its control) were placed 4 cm apart in each box. Then, 7-day-old starved (food not provided for 24 h before assays) or non-starved flies were released into boxes to be exposed to stimuli in an artificial climate chamber (25 °C, 70% relative humidity, 12 h light:12 h dark cycle). The number of flies inside and outside the traps was counted and response indices calculated as described for *D. melanogaster* larvae. Over 60% of adults responded following 24 h of exposure. As no difference in response to the *M. robertsii*-colonized *G. mellonella* cadavers was found between starved and non-starved flies, we report only on assays using starved adult flies with 24 h of exposure as previously described[52].

Analysis of attractiveness of *M. robertsii*-colonized *G. mellonella* cadavers to *G. mellonella* larvae

A modified two-choice assay was developed to analyse the response of healthy *G. mellonella* larvae to *M. robertsii*-colonized *G. mellonella* cadavers versus freeze-killed healthy *G. mellonella* larvae. A transparent plastic box (26 cm × 12 cm × 23 cm) was subdivided into three equal compartments using two transparent boards each with a hole (5 cm × 4 cm) at the bottom to allow insects to travel between compartments (Supplementary Fig. 5c). Two 3-cm Petri dishes (one with seven *Metarhizium*-colonized *G. mellonella* cadavers, one with seven freeze-killed healthy *G. mellonella* larvae) were placed at opposite corners of the box. Forty *G. mellonella* larvae were released into the middle compartment, and the box was placed in the dark at 26 °C for 2 h when over 60% of the insects had made a choice. The number of insects in each compartment was counted and response indices calculated as described for *D. melanogaster* larvae.

Analysis of attractiveness of *M. robertsii*-colonized *G. mellonella* cadavers to wasps, tobacco whiteflies and solenopsis mealybugs

For adults of tobacco whiteflies (*B. tabaci*), solenopsis mealybugs (*P. solenopsis*) and adult wasps (*L. boulardi*), a modified two-choice assay method was used to analyse their responses to *M. robertsii*-colonized *G. mellonella* cadavers (Supplementary Fig. 5d). Single *M. robertsii*-colonized *G. mellonella* cadavers and freeze-killed healthy *G. mellonella* larvae were placed in two 3-cm Petri dishes each with a square entry hole (side = ~1 cm) located at either end of a 15-cm Petri dish. Approximately 20 adult wasps, whiteflies or mealybugs were released in the middle (release point) of the large dish. Insects in the small Petri dishes were counted after 30 min for wasps, and after 6 h for whiteflies and solenopsis mealybugs, when most had made a choice. Response indices were calculated as described above for *D. melanogaster* larvae.

Analysis of mosquito behavioural preference in two-port olfactometer assays

Two-port olfactometer assays were conducted to analyse the behavioural preferences of adult mosquitoes[53]. The olfactometer (Supplementary Fig. 5e) was fabricated in-house according to the literature[53]. Two transparent PVC cylindrical chambers (10 cm long, 9 cm in diameter) were at opposite ends of the two-port olfactometer. When assaying the attractiveness of a stimulus to mosquitoes versus its control (Supplementary Table 3), the stimulus and its control were placed in the two chambers for mosquitoes to choose between, and the response index was calculated using the $(O-C)/T$ method (as described above for *D. melanogaster* larvae). When comparing two stimuli, they were placed in the chambers for mosquitoes to choose between, and behavioural preference was calculated using the N1 or N2/(N1 + N2) method (as described above for *D. melanogaster* larvae). Three transparent PVC tubes (12.5 cm long and 2 cm in diameter) were used to connect the two stimuli-containing chambers. The middle tube with four air outlets (diameter = 1 mm) in the centre was removable and used to introduce ~15 7-day-old adult mosquitoes provided only with water for 12 h before the assays (12 h of sugar starvation). For the first hour, cheesecloth localized mosquitoes in the middle tube for acclimatization. After the cheesecloth was removed, the whole device was placed in an artificial climate incubator at 26 °C for 30 min, during which time filtered, clean airflow (1 l min^{-1}) from an air pump (Tai An Bai Heng Biotechnology) passed through the odour sources. The number of mosquitoes in each chamber was counted to calculate the response index (a stimulus versus its control) or behavioural preference (two stimuli were compared) as described above. The olfactometer was cleaned with 70% ethanol between experiments and replicates.

Observing the fate of ingested spores by *G. mellonella* larvae

Single healthy *G. mellonella* larvae and *G. mellonella* larval cadavers colonized with the *M. robertsii* strain GFP-WT were placed on opposite sides of Petri dishes (diameter = 15 cm) and kept at 26 °C for 30 min. This method was also applied in assays of infection of *G. mellonella* larvae after exposures to the *M. robertsii*-colonized *G. mellonella* cadavers of different ages. After exposure, any spores loosely attached to healthy insects were removed by surface cleaning and sterilization in several changes of sterile TritonX-100 solution (0.05%), 75% ethanol and 1% sodium hypochlorite (NaOCl), with final washing in sterile Triton

X-100 solution (5 times, 1 min each). This last wash was plated onto *Metarhizium*-selective medium[44]; the absence of colony-forming units (CFUs) confirmed the removal of loosely attached spores. Some spores remained attached to intersegmental membranes but were killed during the body surface sterilization (Extended Data Fig. 1c). After surface sterilization, insects were incubated individually in sterilized plastic cups without diet and with ventilation holes. To analyse spores in faeces, faecal pellets were aseptically collected daily. The presence and germination of GFP-labelled spores in faeces were observed using fluorescence microscopy. To quantify spores, faeces were homogenized in sterile Triton X-100 solution and spread onto *Metarhizium*-selective medium. CFUs in faeces released per insect per day were recorded for 6 days after surface sterilization.

To examine spore behaviour in guts, at 0 h, 24 h, 48 h, 72 h and 96 h post-exposure to cadavers, *G. mellonella* larvae were dissected (9 insects per time point) and guts removed. Each gut was rinsed three times in sterile water and sectioned longitudinally. For histological investigations, excised foreguts were fixed for 24 h in a 4% formaldehyde solution, dehydrated for 24 h in a 30% sucrose solution, embedded in OCT agent (SAKURA) and frozen. A Thermo Fisher Scientific HM 550 Cryostat was used at −18 °C to transect 15-µm-thick slices for examination by fluorescence microscopy.

Quantification of spores attached to insect cuticle

To quantify spores attached to the cuticles of larval *G. mellonella* and *D. melanogaster*, single insects were immersed in 2 ml (*G. mellonella*) or 100 µl (*D. melanogaster*) of sterile 0.05% Triton X-100 solution and vortexed for 90 s. The suspension was serially diluted, and 100 µl of each dilution was plated onto *Metarhizium*-selective medium (in 9-cm Petri dishes). The number of spores on an insect was calculated from CFU counts 3 days to 4 days later. For mosquitoes, single adults were placed in a 1.5-ml tube with 100 µl of Triton X-100 solution and manually homogenized with a sterile plastic pestle. The mixture was then evenly spread on the *Metarhizium*-selective medium (in 9-cm Petri dishes) for CFU counts.

Virulence assays with insects inoculated with spore suspensions

Topical inoculation of *G. mellonella* larvae was performed by immersing insects in a spore suspension (3×10^7 spores per ml)[44]. Insects were then individually placed in a small ventilated plastic cup and incubated at 26 °C (90% relative humidity). Dead insects were surface sterilized with NaOCl solution (1%) for 1 min, washed with several changes of sterilized water, placed on sterilized glass slides and incubated at 26 °C in Petri dishes each containing a wet cotton ball to encourage fungal emergence. Death from fungal infection was confirmed by mycelial emergence from cadavers and used to calculate fungal infection-caused LT_{50} and mortality. Confirming death by mycosis in this manner applies to all bioassays using *G. mellonella*, *D. melanogaster* and the three mosquito species.

For mosquito assays, approximately 30 adults per replicate were immobilized at 4 °C for 10 min, then transferred to a white filter paper in a 9-cm Petri dish sitting on ice. Mosquitoes were topically inoculated with 6 squirts of a spore suspension (1×10^5, 1×10^6 or 1×10^7 spores per ml) using a perfume spray, achieving inoculum loads of ~1, ~10 or ~20 spores per mosquito (Extended Data Fig. 7b), respectively. Immediately after inoculation, the Petri dish was placed in a cup covered with mosquito netting with a 10% sucrose solution supplied in a cotton ball sitting on the netting. The cup was incubated at 26 °C at ~90% relative humidity. Mortality was recorded daily. To assay spore yield per mycosed mosquito cadaver, single cadavers were immersed in 500 µl of sterile 0.05% Triton X-100 solution and vortexed for 2 min. The spore concentration was determined using a haemocytometer for calculation of the number of spores per cadaver.

All bioassays were repeated three to six times. LT_{50} and LD_{50} (the number of spores needed to kill 50% of insects) were calculated using GraphPad Prism 7.0.

Assays of mortality of *D. melanogaster* larvae caused by olfaction-induced insect attraction to *Metarhizium*-colonized *G. mellonella* cadavers

Attraction assays of *D. melanogaster* larvae (3rd instar) to *Metarhizium*-colonized *G. mellonella* cadavers were conducted in 9-cm Petri dishes containing 2% water agar. Single cadavers and ~20 larvae were placed on opposite sides of the dishes. After 10 min of exposure, larvae were individually transferred to 3-cm Petri dishes (1 per dish) containing 2% water agar covered with a thin layer of fly food (without fungicides). Fungal infection-caused mortality was recorded daily.

Preparation of samples for VOC emission assays with SPME–GC–MS

We used 4 mycosed *G. mellonella* cadavers and either 1 or 50 mycosed mosquito cadavers per VOC emission assay using solid-phase microextraction–gas chromatography–mass spectrometry (SPME–GC–MS). Fully sporulated BRH cultures (containing mycelium and the medium) were assayed (1 g (wet weight) per assay). Healthy *G. mellonella* larvae were freeze-killed by 10 min of incubation at −20 °C, then kept at room temperature for 2 h before VOC emission assays (4 dead insects per assay).

For fungal mycelium only, fully sporulated mycelium (0.05 g) separated from 12-day cadavers and 14-day-old fully sporulated PDA cultures were assayed. Non-sporulated mycelium collected from liquid medium SDY (cultured for 48 h) was also assayed. Lipid droplets prepared from spores collected from 50 12-day cadavers were used per assay.

For Mexican petunia, five flowers (~1 g in total) or young leaves (~1 g in total) were used per assay.

All VOC emission assays were repeated at least three times.

Profile of VOCs using SPME–GC–MS

VOCs were analysed by SPME–GC–MS as previously described[54]. Briefly, samples were placed in 25-ml glass vials containing an SPME fibre (50/30 µm DVB/CAR/PDMS). After 1 h at 45 °C, VOCs absorbed by the fibre were analysed by GC (Thermo Fisher Scientific) coupled with MS (Agilent) using helium as the carrier gas at a constant velocity of 1 ml min^{-1}. All VOCs from the fibre were injected in splitless mode. A non-polar DB-5 MS column (30 m × 0.25 mm, 0.25 µm; Agilent) or a polar TR-WAX MS column (30 m × 0.25 mm, 0.25 µm; Thermo Fisher Scientific) was used. The temperature in the GC oven started at 40 °C for 2 min and was raised at 5 °C min^{-1} to 180 °C, followed by 10 °C min^{-1} to 270 °C, which was held constant for 10 min. The MS was run in electron impact mode at 70 eV with a scan range of 35–450 mz^{-1}. VOCs corresponding to peaks were predicted by comparing their electron ionization mass spectra with the MS databases (National Institute of Standards and Technology). The identity of a VOC was further confirmed by comparing its retention index with that of its authentic standard, and, if available, previously reported ones. *N*-alkanes (C7–C40) were assayed under the same operating conditions for calculating VOC retention indices using a standard formula[55]. All authentic VOC standards and alkanes were directly injected on both polar and non-polar columns. (+)-Longifolene (CAS: 475-20-7), (+)-sativene (CAS: 3650-28-0), (−)-geosmin (CAS: 19700-21-1), isolongifolene (CAS: 1135-66-6) and 1-octen-3-ol (CAS: 3391-86-4) were purchased from Sigma-Aldrich. The mixture of *n*-alkanes (C7–C40) was purchased from Yuanye Bio-Technology.

For quantification of a VOC, we prepared its standard curve using a series of solutions of the VOC in hexane (range of 0.1–0.6 ng)[54]. The standard curve was created with the VOC amount (*x* axis) plotted against peak areas from the GC analysis (*y* axis).

The percentage of a VOC among total volatiles emitted by a sample was calculated by dividing its peak area by the sum of all VOC peak areas[54].

Lipid droplet staining and preparation

Lipid droplets in spores were stained with BODIPY dye[56]. Stained lipid droplets were observed under a confocal microscope (Zeiss). The stained spores were also analysed by flow cytometry (Beckman Coulter) with CytExpert Software 2.4; 50,000 spores were collected for fluorescence analysis at the emission maxima of 488 nm (ref. 56).

Spore lipid droplets were prepared as previously described with minor modifications[57]. Briefly, spores were disrupted under pressure with a French press cell at 1,500 bar and suspended in HEPES buffer (pH 7.4) containing 20 mM HEPES (Aladdin), 100 mM KCl and 2 mM $MgCl_2$. After vortexing, the sample was centrifuged at 4 °C (10 min at 3,000 × *g*). The supernatant was subjected to ultracentrifugation at 4 °C (1 h at 182,000 × *g*) and lipid droplets were pipetted from the top layer for further analysis. The integrity of lipid droplets was assayed by staining with BODIPY.

To quantify longifolene in lipid droplets, lipid droplets were weighed and applied to a three-layer filter paper (diameter = 1 cm), which was then subjected to SPME–GC–MS analysis as described above. This assay was repeated three times.

Homozygote mutant construction by CRISPR–Cas9

The *Or43b* and *Or74a* mutant lines were generated using the CRISPR–Cas9 system. Two target sites for single guide RNAs (sgRNA1: 5′-TAAGTACTGCGTGAAGCCGG-3′ and sgRNA2: 5′-GAAGCGCAAGGTTCGCGACA-3′) were selected on the Exon 1 of *Or43b*. Two target sites for sgRNAs (sgRNA1: 5′-TACAGACCCCGTCTCCCCGG-3′ and sgRNA2: 5′-CGGTACAAGGACACCGGCCA-3′) were also selected on the Exon 1 of *Or74a*. The protospacer adjacent motif sequences for sgRNA1 and sgRNA2 of *Or43b* are CGG and TGG, respectively, while sgRNA1 and sgRNA2 of *Or74a* have the same protospacer adjacent motif sequence of CGG. The DNA template for each sgRNA was obtained by PCR amplification using long forward primers with a specific T7 promoter sequence (TAATACGACTCACTATAG) as a 5′ extension followed by the sgRNA sequence and a 3′ binding region to the gRNA scaffold (GTTTTAGAGCTAGAAATAGC), along with a common reverse primer. The primers used in this experiment (forward primers: DmOr43b-F1, DmOr43b-F2, DmOr74a-F1 and DmOr74a-F2; reverse primer: sgRNA-R) and the sequences of DNA templates are listed in Supplementary Table 2. PCR products were used for transcription in vitro with the T7 RiboMAX Kit (Promega), and the sgRNA were purified by phenol–chloroform extraction and isopropanol precipitation. The Cas9-expressing plasmid MLM3613 (Addgene) was linearized with the restriction enzyme *Pme* I (NEB), and Cas9 mRNA was then transcribed using the mMESSAGE mMACHINE T7 Ultra Transcription Kit (Ambion), polyadenylated with the *E. coli* Poly(A) Polymerase Kit (NEB), and purified with the RNeasy Mini Kit (QIAGEN).

A mixture of 7.5 μg sgRNA and 15 μg Cas9 mRNA was injected into freshly laid *Drosophila* eggs (w^{1118} strain, BL#5905), which were immediately returned to a 25 °C incubator to allow development into adults as the initial generation (G0). The G0 male adults from injection with *Or43b* sgRNAs were individually crossed with virgin females of *Bc/CyO* balancer flies, and the G0 male adults from injection with *Or74a* sgRNAs were individually crossed with virgin females of *TM3/TM6* balancer flies. Both G0 and G1 generations were genotyped by PCR amplification using a pair of specific primers (Supplementary Table 2), and the generated PCR products were sequenced to examine the mutations. G1 mutant individuals were further crossed with *Bc/CyO* or *TM3/TM6* balancer flies to generate the homozygous mutants for *Or43b* and *Or74a*.

SSR

The coding sequences for *Drosophila* odorant receptors Or43b and Or74a were amplified from larval cDNA using a pair of specific primers with *Kpn* I site (Supplementary Table 2). The pUAST-attB vector plasmid was digested with *Kpn* I (NEB) and recombined with the amplified PCR fragments using the ClonExpress II One Step Cloning Kit (Vazyme). These constructs were purified by the HiSpeed Plasmid Midi Kit (QIAGEN) and injected into *D. melanogaster* (BDSC-25709) embryos for targeted integration into the attP site on chromosome 2 (cytological locus 25C6). Transgenic flies carrying these *UAS-Or* constructs were crossed with *Or67d*^{GAL4} (genotype: *w; Sp/CyO; Or67d*^{GAL4}) flies. Sibling cross was used to produce two *UAS-Or;Or67d*^{GAL4} homozygous flies for *Or43b* (*UAS-Or43b;Or67d*^{GAL4}) and *Or74a* (*UAS-Or74a;Or67d*^{GAL4}).

SSR was performed as previously described with minor modifications[58]. Briefly, male flies (7–10 days old) were individually immobilized in 200-μl plastic pipette tips (Axygen) with the head and antennae protruding and fixed using plasticine under a stereomicroscope. A glass electrode (World Precision Instruments) was inserted into one compound eye as a reference, and the sharpened recording electrode was inserted into the base of a T1 sensilla of antennae. Longifolene solutions were prepared in hexane at a series of concentrations (10^{-2}, 10^{-3}, 10^{-4}, 10^{-5} g ml^{-1}). To test the response to longifolene, 10 μl of solution was applied to a filter paper (0.5 cm × 3 cm) inserted into a Pasteur pipette (150 mm long, Witeg). Hexane was used as the negative control. A continuous airflow at 30 ml s^{-1} was continuously blown over the antenna using a stimulus controller (CS-55, Syntech) and 300-ms stimulus pulses were delivered through a Pasteur pipette. The recorded signals were amplified through an IDAC interface amplifier (IDAC-4, Syntech) and visualized by Autospike v.3.9 software (Syntech). The response value to a stimulus was calculated as the difference in spike counts between 1 s before and after stimulus delivery. Each fly was used only once, with 10 flies (biological replicates) for each treatment.

Expression profiles of *Or43b* and *Or74a*

Total RNA from the most anterior part of *D. melanogaster* larvae or adult antennae was extracted using FastPure Cell/Tissue Total RNA Isolation Kit-BOX 2 (Vazyme) and then reversely transcribed into cDNA using HiScript II Q RT SuperMix (Vazyme) according to the manufacturer's protocol. Reverse-transcription PCR (RT-PCR) was performed with 2 × Phanta Max Master Mix (Vazyme) to detect *Or43b* and *Or74a* expression. *Actin5C* was used as the reference gene. The primers for RT-PCR analysis are listed in Supplementary Table 2.

RNAi-mediated gene silencing in adult mosquitoes using dsRNA injection

The dsRNA was synthesized from *A. albopictus* adult cDNA using the T7 RiboMAX Express RNAi System Kit (Promega) according to the manufacturer's instructions. Primers to amplify odorant receptor genes (*LOR*, *POR1* and *POR2*), the odorant receptor co-receptor gene (*Orco*) and GFP (control) are listed in Supplementary Table 2. The dsRNA concentration was quantified with a NanoDrop 2000 (Thermo Fisher Scientific). Microinjection of mosquitoes was conducted as described[59]. Briefly, adult females and males (3–5 days old) were injected intrathoracically with 200 nl and 150 nl of dsRNA (3 μg μl^{-1}), respectively, using the Drummond Nanoject III (Drummond Scientific). Two days post-injection, mosquito antennae were dissected for RNA preparation to assay gene knockdown efficiency using quantitative reverse-transcription PCR (qRT-PCR). RNA preparation from mosquito antennae and cDNA synthesis were conducted as described above for *D. melanogaster*. qRT-PCR analysis was performed using the Thunderbird SYBR qPCR mix without ROX (Toyobo). The *eEF1-γ* and *rpS7* genes were used as the reference genes[60]. Relative expression levels were calculated as described[35]. Primers for qRT-PCR analysis are listed in Supplementary Table 2. Behavioural assays were also performed 2 days post-injection.

EAG and GC–EAD assays

EAG recordings were performed as described with minor modifications[61]. Briefly, *A. albopictus* or *D. melanogaster* adults were anaesthetized on ice, heads removed and antennae tip inserted into a recording glass electrode filled with NaCl solution (0.9%). A silver wire inserted into the NaCl solution connected the circuit with a reference electrode attached to the head. Signals passed through a high-impedance amplifier (Combi probe, IDAC 4 data acquisition controller, Syntech) and analysed using customized EAG Pro software (Syntech). Each stimulus solution (10 μl) was applied to a Whatman filter paper (0.5 × 3 cm), inserted into a sterilized pipette tip (Axygen) and delivered via an air stream at 1.8 l min^{-1} with a puff (0.5 s duration, 0.4 l min^{-1}) at 60-s intervals. Longifolene was assayed at a series of concentrations (10^{-4}, 10^{-5}, 10^{-6} and 10^{-7} g). Hexane used for preparing the VOC solutions served as a negative control. 1-Octen-3-ol was a positive control for mosquito EAG assays[15]. Treatment values were calculated by subtracting the negative control (hexane) values from the treatment values. Ten different insects were assayed for each concentration.

GC–EAD assays were conducted to assay antennal response to (+)-longifolene. The GC–EAD system consisted of a gas chromatograph (Agilent 7820A) with an HP-5 capillary column (30 m × 0.32 mm × 0.25 μm, J & W Scientific) and a flame ionization detector coupled to an electroantennographic detector (Syntech). The injector temperature was set at 250 °C. The column temperature was held at 40 °C for 2 min, increased by 5 °C min^{-1} to 150 °C and then by 10 °C min^{-1} to 250 °C, which was held for 5 min. Nitrogen was the carrier gas at 3 ml min^{-1}. The detector temperature was 300 °C. A total of 1 μl of longifolene (10^{-4} g ml^{-1}) was injected into the GC. A Y-shaped glass splitter directed the flow at a 1:1 ratio between the flame ionization detector and the antenna. For EAD preparations, single antennae of either *D. melanogaster* or *A. albopictus* adults were mounted between two glass capillaries filled with NaCl solution (0.9%). Air was cleaned with a CS-55 system (Syntech) and used as the VOC carrier gas at 2 l min^{-1}. Signals from the antennae were amplified by PRG-3 (Syntech), digitized using a data acquisition interface (IDAC 4, Syntech) and analysed with GcEad-1.2.5 software (Syntech). We found that only (+)-longifolene in the commercially purchased synthetic triggered an obvious antennal response from *D. melanogaster* and *A. albopictus* adults, while impurities in the synthetic lacked any activity (Fig. 3f), suggesting that the longifolene synthetic is sufficiently pure for the insect EAG and behavioural assays conducted in this study.

Gene disruption and overexpression

Disruption of *M. robertsii* genes via homologous recombination was performed as previously described[62]. Gene disruption plasmids were constructed using restriction enzyme digestion and ligation based on the master plasmid pPK2-bar-GFP (ref. 62).

To construct a plasmid for overexpression of a gene (MAA_06581 or MAA_08668) in *M. robertsii*, the coding sequence was cloned with PCR and inserted into the EcoRV site in the binary expression plasmid pPK2-sur-GFP-T, so that the gene was driven by the constitutive promoter *Ptef* from *Aureobasidium pullulans*[44]. The primers used for plasmid construction are in Supplementary Table 2.

RNA extraction, RT-PCR and qRT-PCR analysis of *Metarhizium* genes

Total RNA from *Metarhizium* mycelia was prepared using TRIzol reagent (Life Technologies).

cDNAs were synthesized from total RNA using the ReverTra AceqPCR RT Master Mix (Toyobo). The cDNA mixture was diluted 20-fold for regular RT-PCR with the *tef* gene as the internal standard. qRT-PCR analysis was performed as described above for mosquitoes. The *gpd* and *act* genes were used as the reference genes[44].

Construction of transgenic fungal strains expressing the pine *Tps* gene

The *Tps* gene encoding longifolene synthase TPS (GenBank accession number ABV44454) from the *P. sylvestris* pine tree was commercially synthesized according to the codon bias of *M. robertsii* (https://www.kazusa.or.jp/codon/). The codon-optimized sequence of the pine TPS was deposited in GenBank (accession number OQ242380) and is shown in Supplementary Table 2. The TPS coding sequence was inserted into the EcoRV site in the binary expression plasmid pPK2-sur-GFP-T (ref. 44), to produce pPK2-sur-GFP-Tps with *Tps* driven by the constitutive promoter *Ptef*. The plasmid pPK2-sur-GFP-Tps was incorporated into *A. tumefaciens* cells for *M. robertsii* ARSEF2575 and *M. pingshaense* TM1 transformation to produce strains Mr-*Tps* and Mp-*Tps*, respectively. Expression of *Tps* was confirmed by RT-PCR.

Production of *Metarhizium* BRH cultures

M. pingshaense BRH cultures were produced using a liquid–solid biphasic method. The liquid phase used SDY medium, inoculated with spores (10^6 spores per ml) from PDA plates. After 48 h of incubation at 26 °C with shaking at 200 rpm, SDY cultures were mixed with BRH medium at a 1:1 ratio (100 ml SDY culture:100 g solid BRH medium). The mixture was incubated at 26 °C and ~70% relative humidity. Sporulation was completed in about 2 weeks, producing BRH cultures (named as 2-week cultures).

The BRH medium was prepared by mixing two portions. The solid portion contained bran (40%), husks (40%) and rice (20%). The rice was soaked in water for 3 h and steamed. The liquid portion contained glucose (2%), $(NH_4)_2SO_4$ (2%), $NaNO_3$ (2%) and KH_2PO_4 (2%). The solid and liquid components were mixed at a ratio of 1:1 (weight (g) to volume (ml)) and autoclaved at 121 °C for 15 min.

Assaying spore yield, germination and viability

To quantify spore yield, 1 g of BRH cultures was suspended in 0.05% TritonX-100 solution (10 ml) and filtered through a glass fibre filter. The spore concentration was determined using a haemocytometer, and the yield was calculated as the number of spores per gram of culture. Spore yield on PDA plates (spores per cm^2) was determined as previously described[63]. Briefly, 100 μl of spore suspensions (1 × 10^7 spores per ml) was evenly spread on a PDA plate (in a 9-cm Petri dish), which was then incubated at 26 °C for 14 days to allow growth and full sporulation. Three agar plugs were collected with cork borers (diameter = 5 mm) from each plate, and individually suspended in 1 ml of sterile Triton X-100 solution (0.1%). Spores in the solution were then counted using haemocytometers for spore yield calculation. Spore yield assays were repeated three times, with four replicates per repeat.

The GT_{50} (time taken for 50% of spores to germinate) was measured in 1/2 SDY (half strength of the SDY medium)[63]. Spore viability was defined as the percentage of spores germinated (germination rate) in 1/2 SDY by 12 h at 26 °C.

Assaying the ability of *Metarhizium* spores to attract and kill mosquitoes in cubic 1-m^3 cages

We measured the ability of a *Metarhizium* strain to attract and kill mosquitoes based on the inoculation rate, inoculum load (the number of spores per mosquito), LT_{50} and mortality. Laboratory-reared adult mosquitoes (*A. albopictus*, *A. sinensis* and *C. pipiens*), 7–12 days after emergence, were used in all assays conducted in cubic 1-m^3 cages with walls of mosquito netting, which were maintained in a sealed room (Fig. 5d). *Metarhizium* spores were placed on the bottom side of the cages (on the floor of the sealed room). To simulate mosquito behavioural assays in the two-port olfactometery in which mosquitoes needed to fly against a head wind to reach an attractant to reduce the frequency that mosquitoes randomly contacted the attractant (Supplementary Fig. 5e), a bottom-to-top airflow (0.6 l min^{-1}) in this sealed room was provided by a ceiling ventilator (Fig. 5d), so that mosquitoes also needed to fly against a head wind to reach cultures on the bottom side of the cages.

For the black cloth method, 1 × 10^9 spores per ml were suspended in sterile 0.01% Triton X-100 solution. Corn oil purchased from local markets was added to the spore suspensions to a final concentration of 2% or 8% (v/v). Circles of black-cotton cheese cloth (diameter = 15 cm) (Supplementary Fig. 6a) were placed in Petri dishes and sprayed with the oil-formulated spore suspension to 1.4 × 10^5 spores per cm^2. Each impregnated cloth was air-dried for 1 h at room temperature and placed in the cages. The relative humidity in this room was approximately 80%, and the temperature was 22–26 °C. Approximately 30 adult mosquitoes were released into each cage, kept in the dark for 12 h and provided with a cotton pad saturated with water. After 12 h of exposure to the fungal spores, mosquitoes were individually captured, and the number of spores per mosquito was determined as described above to estimate the inoculation rate (0–100%) and inoculum load. To assay killing speed, the mosquitoes were placed into cups covered with mosquito netting (a 10% sucrose solution supplied in a cotton ball sitting on the netting), and incubated at 26 °C (90% relative humidity). Mortality caused by fungal infections was recorded daily. This experiment was repeated three to six times.

Pieces of impregnated black cotton cloth were transferred into a 25-ml glass vial for VOC assays using SPME–GC–MS described above.

The ability of sporulated BRH cultures to attract and kill adult mosquitoes was assayed as described for the black cloth method, except that the cloth was replaced with BRH cultures (10 g) in an uncovered 9-cm Petri dish (surface area ~64 cm^2). Mosquitoes were exposed to BRH cultures in cages for 1 h, 2 h or 12 h.

Assays of the toxicity of longifolene fumigation to mosquitoes

Centers for Disease Control and Prevention (CDC) bottle bioassays were performed to evaluate the toxicity of longifolene to mosquitoes according to the CDC guideline[64] with minor modifications. Briefly, 350-ml glass bottles with screw lids were washed with deionized water three times and then thoroughly dried in an oven (Thermo Fisher Scientific) at 70 °C. Longifolene solutions at a series of concentrations (10 μg ml^{-1}, 1 μg ml^{-1}, 100 ng ml^{-1}, 10 ng ml^{-1} and 1 ng ml^{-1}) were prepared with acetone (Sinopharm Chemical Reagent), and 1 ml solution was pipetted into a bottle. After the bottle was tightly capped, it was manually swirled to make sure its bottom, top and sides were coated by the solution. The lid was then removed, and the bottle was rolled on its side until visible liquid was gone. Ten mosquitoes (*A. albopictus*) were gently transferred into the bottle, which was then tightly capped again. After 12 h of fumigation, mosquitoes in the bottle were considered dead when they can no longer stand. The number of dead mosquitoes was recorded to calculate the mortality (%).

Assays of mosquito visitation to fungal BRH cultures

Mosquito visitation was assayed in a cage (30 cm × 30 cm × 30 cm) with five sides covered with mosquito netting and the top side covered with transparent plastic that allows a camera to video mosquito behaviour on fungal BRH cultures (placed on the bottom side) from outside the cage (Supplementary Fig. 7). Single 7-day-old mosquitoes were first released in the cage. Subsequently, 30 min later, 10 g of fungal BRH culture (in a 9-cm Petri dish) was placed on the centre of the bottom side; the surfaces of the fungal cultures were then continuously recorded for 1 h with a video camera at a focus of 2.7–13 mm (DS-U34W (2.7–13 mm), HIKVISION). By reviewing this video, the number of times single mosquitoes visited the cultures and the cumulative time they spent on the cultures were recorded to show visitation of mosquitoes to the cultures. Each mosquito was used only once, with 15–25 mosquitoes (biological replicates) for each treatment.

Assaying the ability of BRH cultures to attract and kill wild-caught mosquitoes in competition with human and plants in a large room

The ability of sporulated BRH cultures to attract and kill wild-caught adult mosquitoes was assayed at 24–28 °C (70–75% relative humidity) in a large sealed room (6.5 m (length) × 5.5 m (width) × 3 m (height)) (Fig. 6a). The volume of this room (107.25 m^3) is about 12-fold larger than the WHO experimental huts used in west Africa[65]. The walls and ceiling of the room were covered with mosquito netting to prevent mosquitoes from escaping.

Sporulated BRH cultures in six square Petri dishes (25 cm × 25 cm, total surface area 0.375 m^2) containing 250 g of cultures per dish were placed at opposite corners of the floor, and cotton pads soaked in water were supplied (Fig. 6a). Approximately 30 7–12-day-old mated wild-caught *A. albopictus* mosquitoes that had never had a blood meal were released at dusk, and after 12 h of exposure to the fungal cultures, they were individually collected into an aspirator connected to a vacuum, and then transferred into 5-ml tubes. Half of the mosquitoes were used for assaying mortality and LT_{50} values as described above, and the other half were used for determination of inoculation rate and inoculum load. To investigate the impact of competing host odours on the attractiveness of fungal cultures, human volunteers slept in a bed under mosquito netting (2 m (length) × 1.5 m (width) × 1.6 m (height)). For at least a week before the experiments, volunteers had not used any cream and perfume, had not eaten greasy and spicy food, and had used scent-free soap; within 24 h of the experiments, volunteers had not taken showers. The bed was placed at the centre of the room, and two healthy male volunteers (23 and 25 years old) took turns sleeping on it. The volunteers went to bed before the mosquitoes were released at dusk and left the bed after the mosquitoes were caught the next morning. The use of human volunteers in this study was approved (approval code: JIPD-2023-015) by the Ethics Committee of Jiangsu Institute of Parasitic Diseases. Signed informed consent was obtained from the volunteers.

Mosquito-attracting flowering Mexican petunia plants were used to investigate the competitive impacts of plant scents on the attractiveness of fungal cultures. Three different pots of flowering Mexican petunias, approximately 1 m tall with 10–12 branches with a total of 4 or 5 flowers, were alternately placed at the centre of the room. To prepare sugar-starved mosquitoes for comparison with fed mosquitoes, 7–12-day-old adults were deprived of sugar solution for 24 h. These experiments were repeated at least three times.

Statistical analysis

The Shapiro–Wilk test was used to check data normality. For non-normal data, Kruskal–Wallis test followed by Dunn's multiple-comparison test evaluated differences among multiple treatments, while two-tailed Mann–Whitney test calculated differences between two treatments. For normally distributed data, parametric two-tailed Student's *t*-test calculated the differences between two treatments, and one-way ANOVA followed by Tukey's multiple-comparison test was used for multiple treatments. Insect survival rates were shown as Kaplan–Meier curves and analysed with log-rank tests. Correlation coefficients and two-tailed *P* values were calculated with Pearson's correlation for normally distributed data and Spearman's rank correlation for non-normal data. For all statistical tests, *P* values were set as $^{*}P < 0.05$, $^{**}P < 0.01$, $^{***}P < 0.001$ and $^{****}P < 0.0001$ with a 95% confidence interval. All analyses were performed using GraphPad Prism 7.0.

Reporting summary

Further information on research design is available in the Nature Portfolio Reporting Summary linked to this article.

Data availability

All data that support the findings of this study are available in the article and Supplementary Information. The codon-optimized sequence of the pine longifolene synthase TPS was deposited in GenBank (accession number OQ242380). Source data are provided with this paper.

References

1. *World Malaria Report* (World Health Organization, 2024); https://www.who.int/teams/global-malaria-programme/reports/world-malaria-report-2024
2. Farenhorst, M. et al. Fungal infection counters insecticide resistance in African malaria mosquitoes. *Proc. Natl Acad. Sci. USA* **106**, 17443–17447 (2009).

3. Bilgo, E. et al. Improved efficacy of an arthropod toxin expressing fungus against insecticide-resistant malaria-vector mosquitoes. *Sci. Rep.* **7**, 3433 (2017).
4. Lovett, B. et al. Transgenic *Metarhizium* rapidly kills mosquitoes in a malaria-endemic region of Burkina Faso. *Science* **364**, 894–897 (2019).
5. Barrera, R. New tools for *Aedes* control: mass trapping. *Curr. Opin. Insect Sci.* **52**, 100942 (2022).
6. Lwetoijera, D. W. et al. An extra-domiciliary method of delivering entomopathogenic fungus, *Metarhizium anisopliae* IP 46 for controlling adult populations of the malaria vector, *Anopheles arabiensis*. *Parasit. Vectors* **3**, 18 (2010).
7. Angelone, S., Piña-Torres, I. H., Padilla-Guerrero, I. E. & Bidochka, M. J. "Sleepers" and "Creepers": a theoretical study of colony polymorphisms in the fungus *Metarhizium* related to insect pathogenicity and plant rhizosphere colonization. *Insects* **9**, 104 (2018).
8. George, J., Jenkins, N. E., Blanford, S., Thomas, M. B. & Baker, T. C. Malaria mosquitoes attracted by fatal fungus. *PLoS ONE* **8**, e62632 (2013).
9. St. Leger, R. J. & Wang, J. B. *Metarhizium*: jack of all trades, master of many. *Open Biol.* **10**, 200307 (2020).
10. Kant, M. R., Ament, K., Sabelis, M. W., Haring, M. A. & Schuurink, R. C. Differential timing of spider mite-induced direct and indirect defenses in tomato plants. *Plant Physiol.* **135**, 483–495 (2004).
11. Morteza-Semnani, K., Saeedi, M. & Akbarzadeh, M. Essential oil composition of *Teucrium scordium* L. *Acta Pharm.* **57**, 499–504 (2007).
12. Larsson, M. C. et al. Or83b encodes a broadly expressed odorant receptor essential for *Drosophila* olfaction. *Neuron* **43**, 703–714 (2004).
13. Sweeney, S. T., Broadie, K., Keane, J., Niemann, H. & O'Kane, C. J. Targeted expression of tetanus toxin light chain in *Drosophila* specifically eliminates synaptic transmission and causes behavioral defects. *Neuron* **14**, 341–351 (1995).
14. Elmore, T., Ignell, R., Carlson, J. R. & Smith, D. P. Targeted mutation of a *Drosophila* odor receptor defines receptor requirement in a novel class of sensillum. *J. Neurosci.* **23**, 9906–9912. (2003).
15. Takken, W. & Knols, B. G. J. Odor-mediated behavior of Afrotropical malaria mosquitoes. *Annu. Rev. Entomol.* **44**, 131–157 (1999).
16. Paixão, F. R. S. et al. Pathogenicity of microsclerotia from *Metarhizium robertsii* against *Aedes aegypti* larvae and antimicrobial peptides expression by mosquitoes during fungal–host interaction. *Acta Trop.* **249**, 107061 (2024).
17. Hassan, J. et al. Engineered *Saccharomyces cerevisiae* for the de novo synthesis of the aroma compound longifolene. *Chem. Eng. Sci.* **226**, 115799 (2020).
18. Gao, Q. et al. Genome sequencing and comparative transcriptomics of the model entomopathogenic fungi *Metarhizium anisopliae* and *M. acridum*. *PLoS Genet.* **7**, e1001264 (2011).
19. Lovett, B. et al. Behavioral betrayal: how select fungal parasites enlist living insects to do their bidding. *PLoS Pathog.* **16**, e1008598 (2020).
20. de Bekker, C., Beckerson, W. C. & Elya, C. Mechanisms behind the madness: how do zombie-making fungal entomopathogens affect host behavior to increase transmission? *mBio* **12**, e0187221 (2021).
21. Brancini, G. T. P., Hallsworth, J. E., Corrochano, L. M. & Braga, G. Ú. L. Photobiology of the keystone genus *Metarhizium*. *J. Photochem. Photobiol. B* **226**, 112374 (2022).
22. Behie, S. W., Zelisko, P. M. & Bidochka, M. J. Endophytic insect-parasitic fungi translocate nitrogen directly from insects to plants. *Science* **336**, 1576–1577 (2012).
23. Melo, N. et al. Geosmin attracts *Aedes aegypti* mosquitoes to oviposition sites. *Curr. Biol.* **30**, 127–134 (2020).
24. Stensmyr, M. C. et al. A conserved dedicated olfactory circuit for detecting harmful microbes in *Drosophila*. *Cell* **151**, 1345–1357 (2012).
25. Hallem, E. A., Ho, M. G. & Carlson, J. R. The molecular basis of odor coding in the *Drosophila* antenna. *Cell* **117**, 965–979 (2004).
26. Wang, Q. et al. Identification of multiple odorant receptors essential for pyrethrum repellency in *Drosophila melanogaster*. *PLoS Genet.* **17**, e1009677 (2021).
27. Kreher, S. A., Kwon, J. Y. & Carlson, J. R. The molecular basis of odor coding in the *Drosophila* larva. *Neuron* **46**, 445–456 (2005).
28. Marshall, B., Warr, C. G. & de Bruyne, M. Detection of volatile indicators of illicit substances by the olfactory receptors of *Drosophila melanogaster*. *Chem. Senses* **35**, 613–625 (2010).
29. Konopka, J. K. et al. Olfaction in *Anopheles* mosquitoes. *Chem. Senses* **46**, bjab021 (2021).
30. Tusting, L. S. et al. Housing improvements and malaria risk in sub-Saharan Africa: a multi-country analysis of survey data. *PLoS Med.* **14**, e1002234 (2017).
31. *Guidelines for Efficacy Testing of Spatial Repellents* WHO/HTM/NTD/WHOPES/2013 (World Health Organization, 2013).
32. Moonjely, S. & Bidochka, M. J. Generalist and specialist *Metarhizium* insect pathogens retain ancestral ability to colonize plant roots. *Fungal Ecol.* **41**, 209–217 (2019).
33. Wang, J. B., Lu, H. L., Sheng, H. & St. Leger, R. J. A *Drosophila melanogaster* model shows that fast growing *Metarhizium* species are the deadliest despite eliciting a strong immune response. *Virulence* **14**, 2275493 (2023).
34. Ngugi, H. K. & Scherm, H. Mimicry in plant-parasitic fungi. *FEMS Microbiol. Lett.* **257**, 171–176 (2006).
35. Pull, C. D. et al. Destructive disinfection of infected brood prevents systemic disease spread in ant colonies. *eLife* **7**, e32073 (2018).
36. Api, A. M. et al. RIFM fragrance ingredient safety assessment, longifolene, CAS Registry Number 475-20-7. *Food Chem. Toxicol.* **134**, 110823 (2019).
37. Mukai, A., Takahashi, K. & Ashitani, T. Antifungal activity of longifolene and its autoxidation products. *Eur. J. Wood Wood Prod.* **76**, 1079–1082 (2018).
38. Ryabchenko, B. et al. Investigation of anticancer and antiviral properties of selected aroma samples. *Nat. Prod. Commun.* **3**, 1085–1088 (2008).
39. Schmidt, E. et al. Antimicrobial activities of single aroma compounds. *Nat. Prod. Commun.* **5**, 1365–1368 (2010).
40. Tsuruta, K. et al. Inhibition activity of essential oils obtained from Japanese trees against *Skeletonema costatum*. *J. Wood Sci.* **57**, 520–525 (2011).
41. Fang, W. & St. Leger, R. J. Enhanced UV resistance and improved killing of malaria mosquitoes by photolyase transgenic entomopathogenic fungi. *PLoS ONE* **7**, e43069 (2012).
42. Tang, X., Wang, X., Cheng, X., Wang, X. & Fang, W. *Metarhizium* fungi as plant symbionts. *New Plant Prot.* **2**, e23 (2025).
43. Fang, W., Pei, Y. & Bidochka, M. J. Transformation of *Metarhizium anisopliae* mediated by *Agrobacterium tumefaciens*. *Can. J. Microbiol.* **52**, 623–626 (2006).
44. Zhang, X., Meng, Y., Huang, Y., Zhang, D. & Fang, W. A novel cascade allows *Metarhizium robertsii* to distinguish cuticle and hemocoel microenvironments during infection of insects. *PLoS Biol.* **19**, e3001360 (2021).
45. Rehner, S. A. Genetic structure of *Metarhizium* species in western USA: finite populations composed of divergent clonal lineages with limited evidence for recent recombination. *J. Invertebr. Pathol.* **177**, 107491 (2020).

46. Tamura, K., Stecher, G., Peterson, D., Filipski, A. & Kumar, S. MEGA6: Molecular Evolutionary Genetics Analysis version 6.0. *Mol. Biol. Evol.* **30**, 2725–2729 (2013).
47. Ronquist, F. & Huelsenbeck, J. P. MrBayes 3: Bayesian phylogenetic inference under mixed models. *Bioinformatics* **19**, 1572–1574 (2003).
48. Huang, J. H., Reilein, A. & Kalderon, D. Yorkie and Hedgehog independently restrict BMP production in escort cells to permit germline differentiation in the *Drosophila* ovary. *Development* **144**, 2584–2594 (2017).
49. Fishilevich, E. et al. Chemotaxis behavior mediated by single larval olfactory neurons in *Drosophila*. *Curr. Biol.* **15**, 2086–2096 (2005).
50. Dweck, H. K. M. et al. The olfactory logic behind fruit odor preferences in larval and adult *Drosophila*. *Cell Rep.* **23**, 2524–2531 (2018).
51. Zhang, H. et al. A volatile from the skin microbiota of flavivirus-infected hosts promotes mosquito attractiveness. *Cell* **28**, S0092-8674(22)00641-9 (2022).
52. Stökl, J. et al. A deceptive pollination system targeting drosophilids through olfactory mimicry of yeast. *Curr. Biol.* **20**, 1846–1852 (2010).
53. Robinson, A. et al. *Plasmodium*-associated changes in human odor attract mosquitoes. *Proc. Natl Acad. Sci. USA* **115**, E4209–E4218 (2018).
54. Xu, Y. et al. Plant volatile organic compound (E)-2-hexenal facilitates *Botrytis cinerea* infection of fruits by inducing sulfate assimilation. *New Phytol.* **231**, 432–446 (2021).
55. Babushok, V. I. Chromatographic retention indices in identification of chemical compounds. *Trends Anal. Chem.* **69**, 98–104 (2015).
56. Song, H. et al. An inactivating mutation in the vacuolar arginine exporter gene *Vae* results in culture degeneration in the fungus *Metarhizium robertsii*. *Environ. Microbiol.* **24**, 2924–2937 (2022).
57. Chen, Y. et al. Nitrogen-starvation triggers cellular accumulation of triacylglycerol in *Metarhizium robertsii*. *Fungal Biol.* **122**, 410–419 (2018).
58. Guo, H. et al. Sex pheromone communication in an insect parasitoid, *Campoletis chlorideae* Uchida. *Proc. Natl Acad. Sci. USA* **119**, e2215442119 (2022).
59. Pan, X. et al. *Wolbachia* induces reactive oxygen species (ROS)-dependent activation of the Toll pathway to control dengue virus in the mosquito *Aedes aegypti*. *Proc. Natl Acad. Sci. USA* **109**, E23–E31 (2012).
60. Zhang, M. et al. Early attainment of 20-hydroxyecdysone threshold shapes mosquito sexual dimorphism in developmental timing. *Nat. Commun.* **16**, 321 (2025).
61. Lahondère, C. A step-by-step guide to mosquito electroantennography. *J. Vis. Exp.* **169**, e62042 (2021).
62. Xu, C. et al. A high-throughput gene disruption methodology for the entomopathogenic fungus *Metarhizium robertsii*. *PLoS ONE* **9**, e107657 (2014).
63. Meng, Y. et al. A novel nitrogen and carbon metabolism regulatory cascade is implicated in entomopathogenicity of the fungus *Metarhizium robertsii*. *mSystems* **6**, e0049921 (2021).
64. Brogdon, W. G. & Chan, A. *Guideline for Evaluating Insecticide Resistance in Vectors Using the CDC Bottle Bioassay* (US Centers for Disease Control and Prevention, 2010); https://stacks.cdc.gov/view/cdc/21777
65. Bayili, K. Laboratory and experimental hut trial evaluation of VECTRON™ T500 for indoor residual spraying (IRS) against insecticide resistant malaria vectors in Burkina Faso. *Gates Open Res.* **6**, 57 (2022).

Acknowledgements

We thank M. Jiang and X. Wang from the Institute of Insect Science at Zhejiang University for providing experimental insects. We thank Y. Chen and Y. Xu at Zhejiang University for help with SPME–GC–MS analysis, D. Lou at Zhejiang University for help with video recording and X. Deng at Nanjing Medical University for help with statistical analysis. We recognize the indispensable efforts of undergraduate students at Zhejiang University involved in this study (H. Jiang, Y. Yang and J. Liu). This work was funded by grants from National Natural Science Foundation of China to W.F. (82261128002, 32172470) and to J. Huang (32325044), Gates Foundation (INV-070892) and 'Pioneer' and 'Leading Goose' R&D Program of Zhejiang (2023C02025) to W.F., and National Key R&D Program of China (number 2023YFA1801004) to J. Cao.

Author contributions

W.F., D.T., J. Huang and R.J.S. designed the study. W.F. and J. Huang supervised the study. D.T., J. Chen, Y.Z., X.T., X.W., X.C., J.Z., W.S., S.L., Q.Z., Y.H. and S.-H.Y. performed the experiments. C.Y., J.N., M.Z., J. Hu, G.Z., E.B. and A.D. provided technical support in the experiments. W.F., D.T., J. Huang, J. Cao and R.J.S. prepared the paper with input from the other authors. All authors contributed to the interpretation of the data and read and approved the final paper.

Competing interests

D.T. and W.F. filed a patent application (Chinese Patent application no. 202210069879.X, published April 27, 2022). The other authors declare no competing interests.

Additional information

Extended data is available for this paper at https://doi.org/10.1038/s41564-025-02155-9.

Supplementary information The online version contains supplementary material available at https://doi.org/10.1038/s41564-025-02155-9.

Correspondence and requests for materials should be addressed to Jun Cao, Raymond J. St. Leger, Jianhua Huang or Weiguo Fang.

Peer review information *Nature Microbiology* thanks Marcio Cortes, Olaf Kniemeyer, Patil Tawidian and the other, anonymous, reviewer(s) for their contribution to the peer review of this work. Peer reviewer reports are available.

https://doi.org/10.1038/s41564-025-02155-9

[1]State Key Laboratory of Vegetation Structure, Function and Construction (VegLab), MOE Key Laboratory of Biosystems Homeostasis and Protection, College of Life Science, Zhejiang University, Hangzhou, China. [2]Institute of Insect Sciences, College of Agriculture and Biotechnology, Zhejiang University, Hangzhou, China. [3]National Health Commission Key Laboratory of Parasitic Disease Control and Prevention, Jiangsu Provincial Key Laboratory on Parasite and Vector Control Technology, Jiangsu Institute of Parasitic Diseases, Wuxi, China. [4]Institut de Recherche en Sciences de la Santé/Centre Muraz, Bobo-Dioulasso, Burkina Faso. [5]Department of Entomology, University of Maryland College Park, College Park, MD, USA. [6]These authors contributed equally: Dan Tang, Jiani Chen, Yubo Zhang. ✉e-mail: caojuncn@hotmail.com; stleger@umd.edu; jhhuang@zju.edu.cn; wfang1@zju.edu.cn

 https://doi.org/10.1038/s41564-025-02155-9

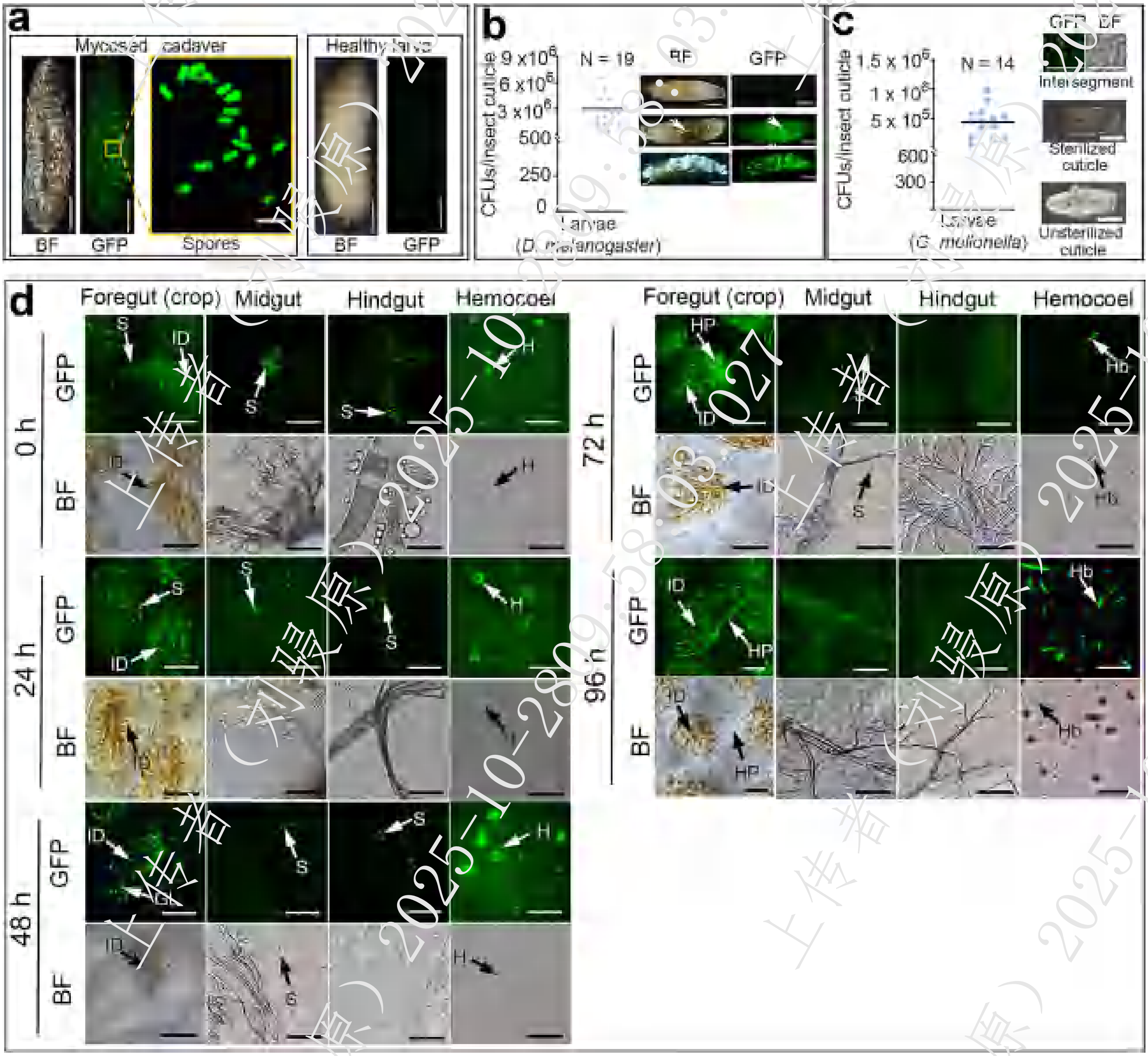

Extended Data Fig. 1 | *M. robertsii*-colonized *G. mellonella* larval cadavers attract healthy insects to become infected. (**a**) *G. mellonella* larva mycosed by the GFP-expressing *M. robertsii* strain *WT-GFP* visualized with bright field (BF, Left, scale bar: 0.5 cm), and epifluorescence using filters set to detect GFP fluorescence (GFP, Middle). *WT-GFP* spores on the cadaver (Right, scale bar: 10 μm). Healthy larvae used as controls for autofluorescence. (**b**) Healthy 3rd instar *D. melanogaster* larvae were infected after attraction to *M. robertsii*-colonized *G. mellonella* cadavers. Left panel: *WT-GFP* CFUs per larval surface after 10 min exposure to cadavers. Right panel: insects after exposure to cadavers (top: healthy larvae as a control for autofluorescence; middle: dark green spores (arrowed) in guts just post-exposure; bottom: a *WT-GFP*-colonized *D. melanogaster* cadaver five days post-exposure). Scale bar: 0.1 cm. N: the number of insects assayed. (**c**) Spores attached to the cuticle of healthy *G. mellonella* larvae after 30 min exposure to *M. robertsii*-colonized *G. mellonella* cadavers. Left: *WT-GFP* CFUs per larval surface. Right: spores and fungal growth on larval cuticle [top: spores attached to intersegmental membranes after body surface sterilization (scale bar: 50 μm); middle: excised cuticle from sterilized insect placed on *Metarhizium*-selective medium (note: no fungal growth); bottom: fungal growth on excised cuticle from unwashed insects (scale bar: 1 cm)]. (**d**) Ingested spores in the alimentary canals of healthy *G. mellonella* larvae at different time points after 30 min exposure to *WT-GFP*-colonized *G. mellonella* cadavers. This figure supplement Fig. 1d. Note: ingested spores can infect healthy larvae by penetrating foreguts. S: spores; GL: fungal germlings; HP: fungal hyphae; H: insect hemocytes. ID: intima dentation in foregut crops; Hb: yeast-like hyphal bodies (blastospores) of the fungus. Scale bar: 50 μm. Images are representative of at least three independent experiments.

 https://doi.org/10.1038/s41564-025-02155-9

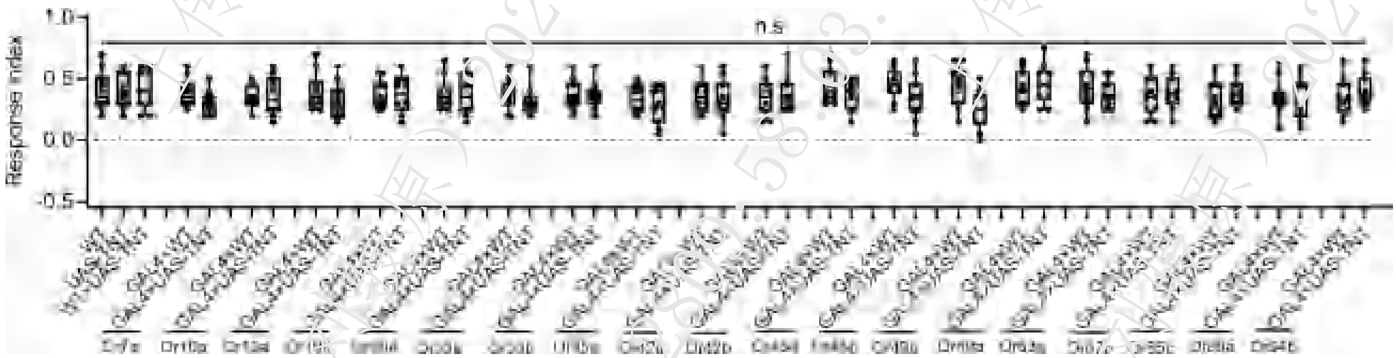

Extended Data Fig. 2 | Two-way choice assays of the response to longifolene (10^{-5} g) (versus hexane) of larvae of the WT (wild type), deficiency lines of 19 larval ORs (constructed with the Or-GAL4/UAS-TNT system), and their respective controls. Response index was calculated as (O-C)/T, where O was the number of larvae in the longifolene zone, C was the number in the hexane (control) zone, and T was the total number of larvae assayed. The box plots show the median (center line), the interquartile range (box bounds, 25th to 75th percentiles), and the whiskers (minima and maxima within 1.5 × interquartile range from the box). n.s: not significantly different ($P > 0.05$, one-way ANOVA with Tukey's multiple-comparison test, n = 10). Data about two other larval deficient lines (Or43b and Or74a) are shown in Fig. 3b. Note: data about WT, UAS-TNT, WT×UAS-TNT are also shown in Fig. 3b for convenient comparison.

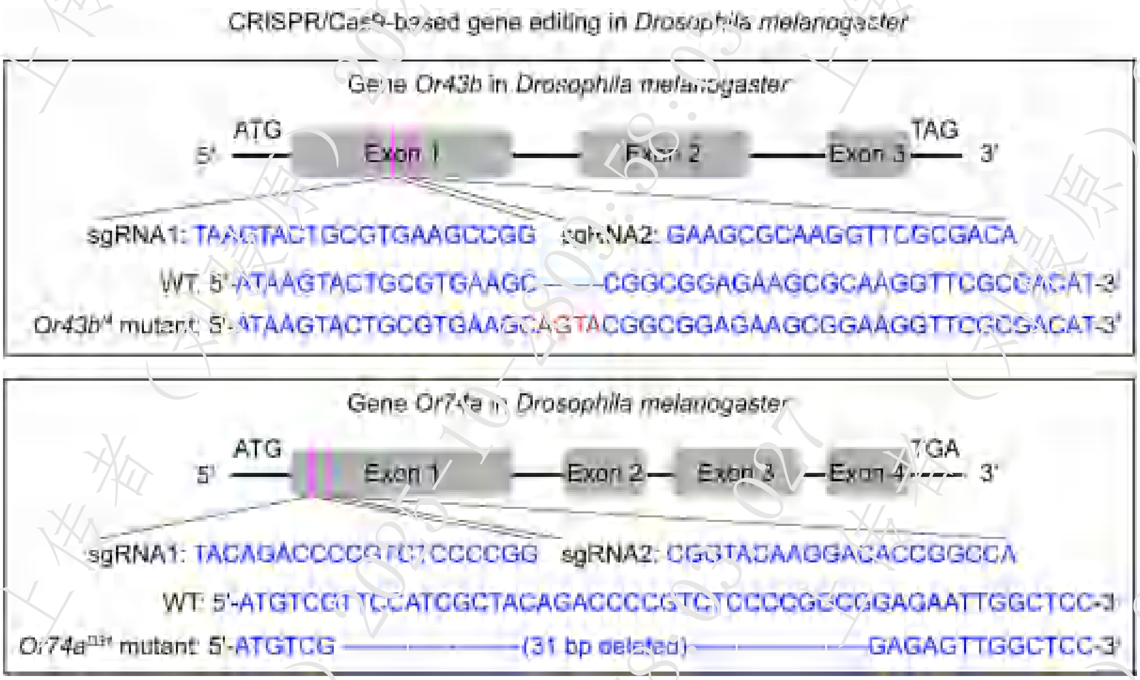

Extended Data Fig. 3 | Generation of the *Or43b* and *Or74* mutant using CRISPR/Cas9-based gene editing. Upper panel: *Or43b* mutant *Or43b*^{I4} with four base pairs (highlighted in red) inserted into Exon 1. Lower panel: *Or74a* mutant *Or74a*^{D31} with 31 base pairs deleted (shown in dashed line) in the Exon 1.

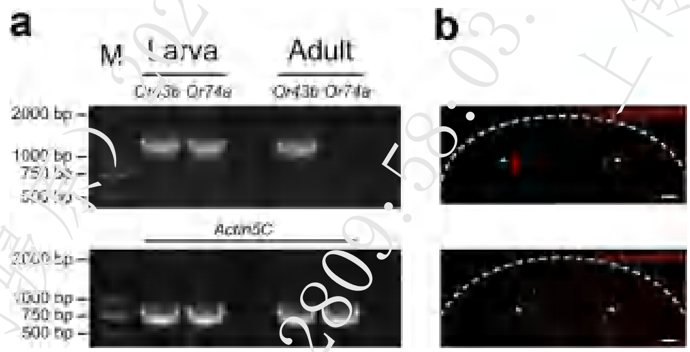

Extended Data Fig. 4 | Expression profiles of *Or43b* and *Or74a* in *D. melanogaster*. (**a**) RT-PCR analysis of *Or43b* and *Or74a* expression in larvae and adult antennae. Larva: total RNA from the most anterior part of the larvae, containing dorsal organ; Adult: total RNA from antennae. M: DNA ladder. *Actin5C*: reference gene. (**b**) Determination of the expression of Or43b and Or74a in larvae via observation of mRFP in a single symmetric pair of larval ORNs (Arrowed), one in each dorsal organ in larvae with mRFP expression driven by *Or43b-GAL4* (genotype: *Or43b > mCD8-RFP*) (Upper panel) and *Or74a-GAL4* (genotype: *Or74a > mCD8-RFP*) (Lower panel). The most anterior part of *Drosophila* larva outlined with white dash line. Scale bars: 20 µm. Images are representative of three independent experiments.

https://doi.org/10.1038/s41564-025-02155-9

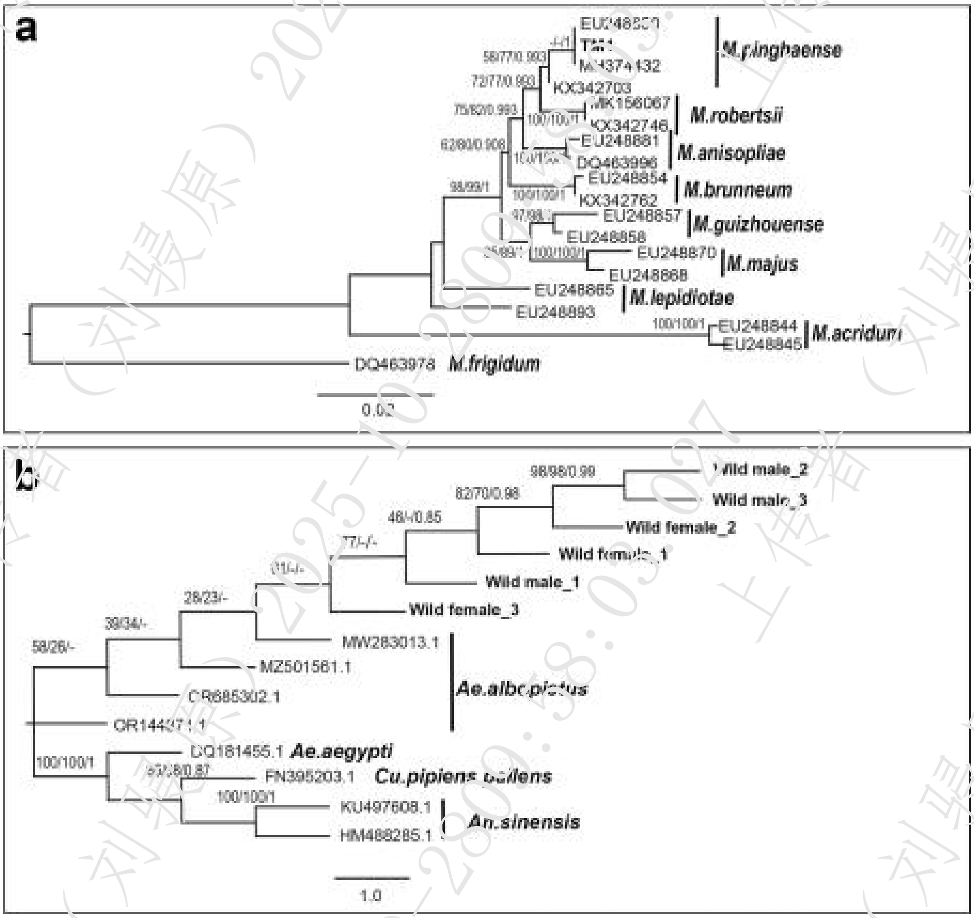

Extended Data Fig. 5 | Phylogenetic analyses identifying the *Metarhizium* isolate used in this study as *M. pingshaense* and the wild-caught mosquitoes as *Ae. albopictus.* (**a**) Analysis of *M. pingshaense* TM1 strain (bold) compared to previously determined *Metarhizium* species using the 5′TEF sequences. The 5′TEF sequence from the TM1 strain is shown in Supplementary Table 2. (**b**) Analysis of three randomly selected wild-caught male and female mosquitoes compared to previously determined *Aedes* species using the *Mt-COI* gene. The GenBank accession number for each sequence from a previously determined species is shown. Numbers at nodes represent the bootstrap values from Neighbor-Joining (left), Maximum Likelihood (middle), and Bayesian posterior probabilities (right). A hyphen (-) indicates no support for the given node in the corresponding method. The scale bar corresponds to the estimated number of nucleotide substitutions per site.

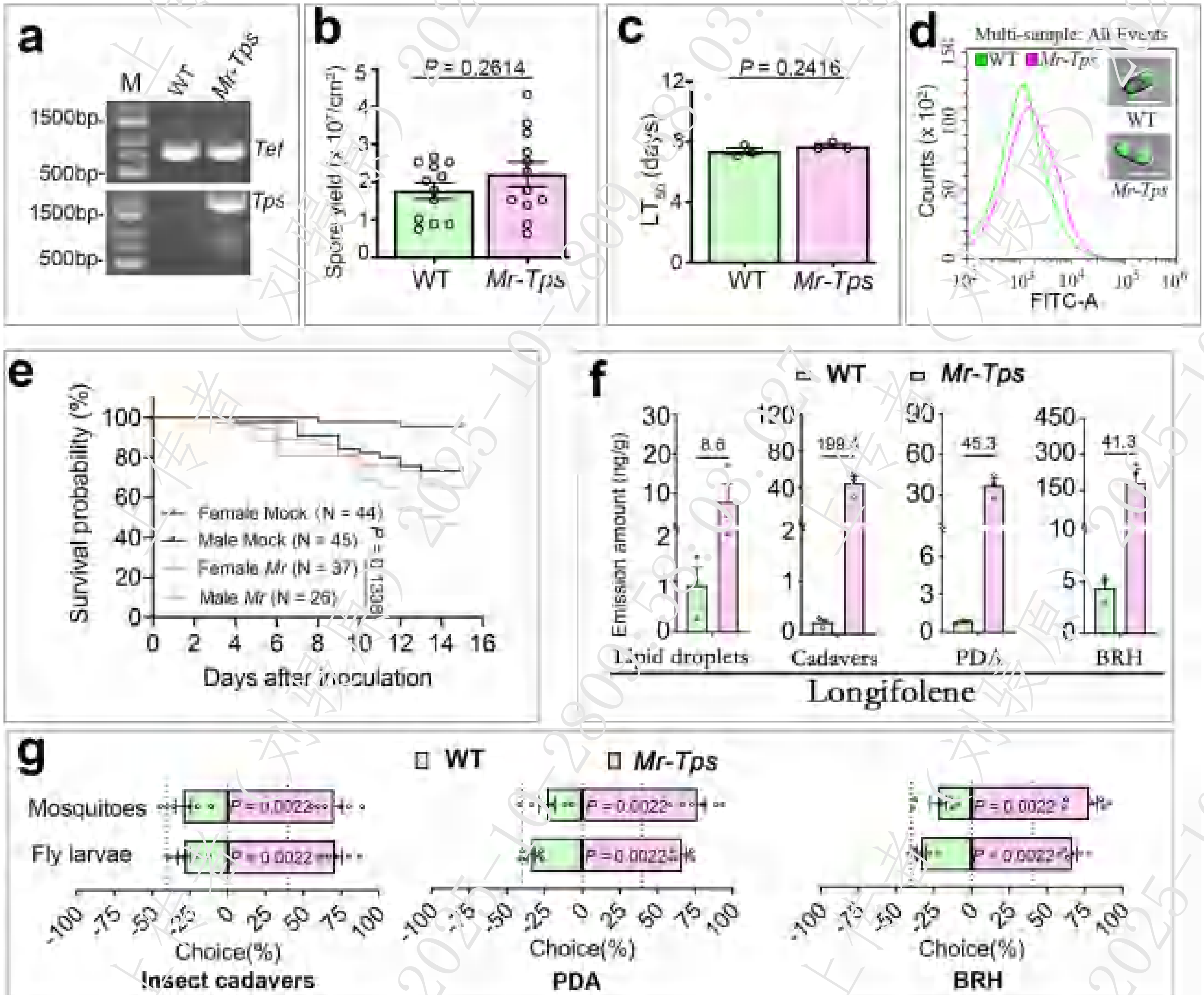

Extended Data Fig. 6 | Construction of transgenic *M. robertsii* strain *Mr-Tps* expressing the pine longifolene synthase gene *Tps* driven by the constitutive *Aureobasidium pullulans* promoter *Ptef*. (**a**) RT-PCR confirmation of *Tps* expression in *M. robertsii*. M: DNA ladder. *Tef*: reference gene encoding translation elongation factor. WT: the parental WT strain of *Mr-Tps*. Images are representative of three independent experiments. (**b**) Spore yield on the PDA. Experiment repeated three times with four replicates per repeat. Two-tailed Student's t-test was used [also used in c in this figure n = 12 (b) and n = 3 (c)]. Data presented as mean ± SE. (**c**) Pathogenicity against *G. mellonella* larvae infected with 3×10^7 spores/mL. Data presented as mean ± SE. (**d**) Flow cytometry assays of spore lipid droplets stained with BODIPY dye. Inset: representative stained spores (of over 100 spores). Scale bar: 5μm. Note: no obvious difference between *Mr* and *Mr-Tps*. (**e**) Kaplan-Meier curves of survival of *Ae. albopictus* adults after being sprayed with *Mr-Tps* spore suspensions (10^7 spores/mL). Log-rank test was used (N: the number of insects assayed). (**f**) Emission of longifolene by lipid droplets from 12-day *M. robertsii*-colonized *G. mellonella* cadavers, sporulated mycelia from the cadavers, PDA and BRH cultures. Values represent fold changes in emission amount of longifolene by *Mr-Tps* compared to the WT. Data presented as mean ± SE. (**g**) Behavioral preferences of *Ae. albopictus* adult female mosquitoes (two-port olfactometer assay) and *D. melanogaster* larvae (two-choice assay) for the WT and *Mr-Tps* spores on mycosed *G. mellonella* cadavers, PDA and BRH. Behavioral preference was shown as the percentage of insects in either stimulus zone out of the total of insects that had made a choice, which was calculated as N1or N2/(N1 + N2), where N1 was the number of insects in stimulus #1 zone, and N2 in stimulus #2 zone. Data presented as mean ± SE. Two-tailed Mann-Whitney test was used (n = 6).

https://doi.org/10.1038/s41564-025-02155-9

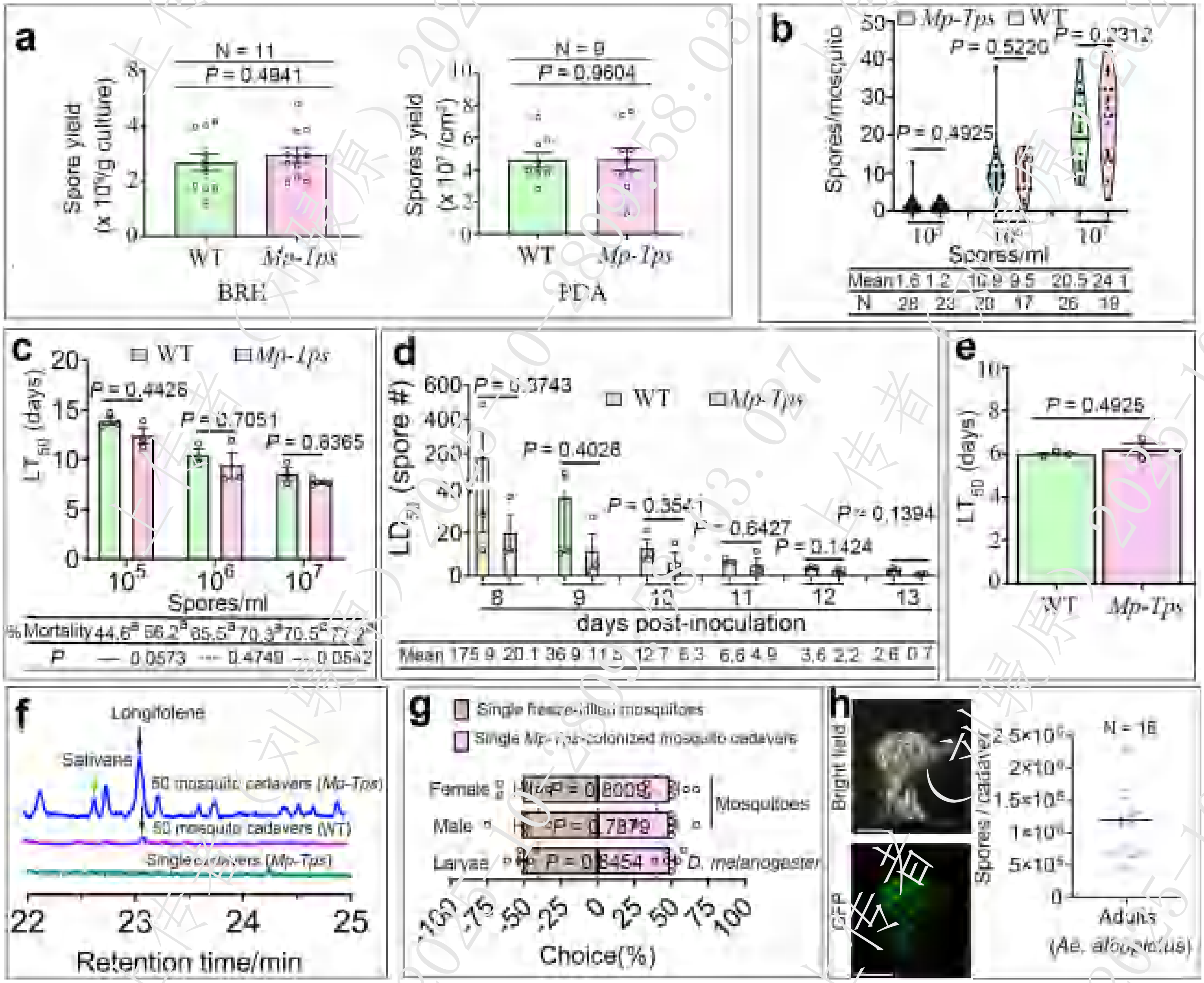

Extended Data Fig. 7 | Characterization of transgenic *M. pingshaense* strain *Mp-Tps* expressing pine longifolene synthase gene *Tps*. (**a**) Spore yields on BRH (left) and PDA (right) media. Two-tailed Student's t-test was used. Data presented as mean ± SE. WT: the parental WT strain of *Mp-Tps*. (**b**) Number of spores per adult mosquito (*Ae. albopictus*) after being sprayed with spore suspensions (10^5, 10^6 or 10^7 spores/mL). Horizontal line: medians. N: the number of mosquitoes assayed. Two-tailed Mann-Whitney test was used. (**c**) LT_{50} values for mosquitoes with inoculations described in (b). Two-tailed Student's t-test was used (n = 3). Data presented as mean ± SE. For mortalities seven days post-inoculation, within each spore suspension, values with same letters are not significantly different (*P* values shown below, Two-tailed Student's t-test, n = 3). (**d**) LD_{50} values for mosquitoes with inoculations described in (b). Two-tailed Student's t-test was used (n = 3). Data presented as mean ± SE. (**e**) LT_{50} values for *G. mellonella* larvae following immersion in 3×10^7 spores/ml. Two-tailed Student's t-test was used. Data presented as mean ± SE. (**f**) Longifolene and sativene-containing portions of GC-MS analysis of 50-, and single *Mp-Tps* or the WT colonized mosquito cadavers. Note: no longifolene detected in single *Mp-Tps* cadavers. (**g**) Behavioral preferences (single *Mp-Tps*-colonized mosquito cadavers versus freeze-killed mosquitoes) of adult *Ae. albopictus* mosquitoes and 3rd instar *D. melanogaster* larvae. Data presented as mean ± SE. Two-tailed Mann-Whitney test was used (n = 6). (**h**) A representative *Mp-Tps*-colonized mosquito cadaver (of over 30 cadavers) under bright field and epifluorescence using filters set to detect GFP fluorescence (GFP) (Left panel), and the number of spores on single cadavers (Right panel). N: the number of mosquitoes assayed. Scale bar: 2 mm.

https://doi.org/10.1038/s41564-025-02155-9

a

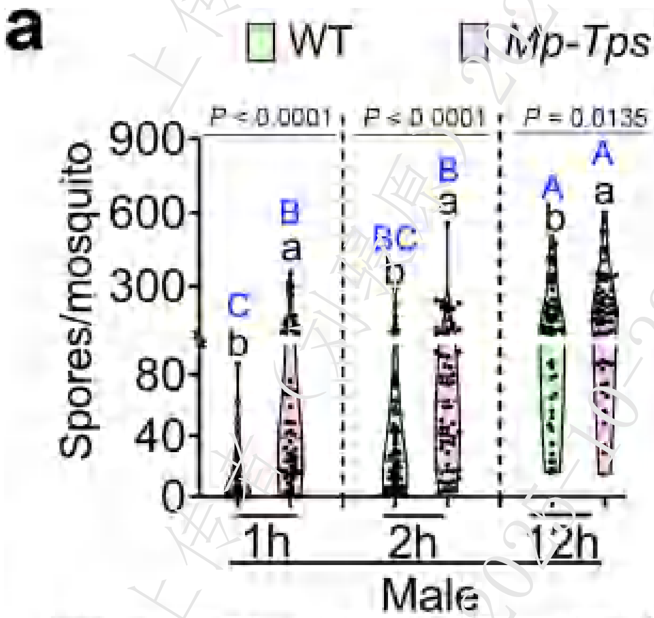

	WT	Mp-Tps	WT	Mp-Tps	WT	Mp-Tps
Mean	12	80	42	87	178	222
Median	5	39	24	63	156	196
%Inoculation	70.3^b	95.4^a	100	100	100	100
N	64	62	64	61	59	61
P-value	---	0.0052	---	---	---	---

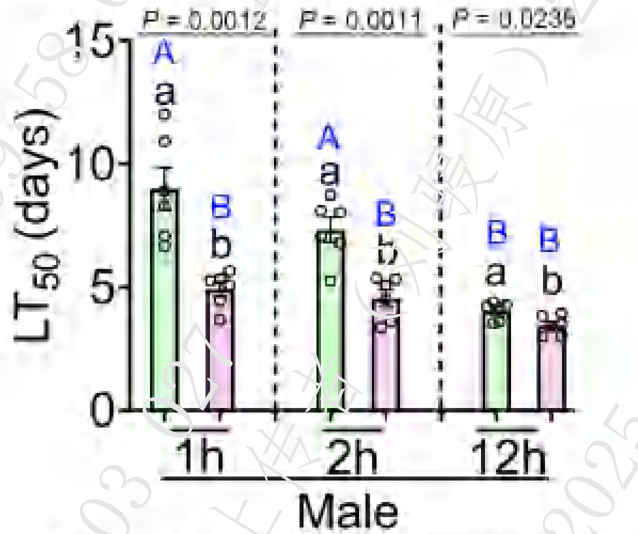

	WT	Mp-Tps	WT	Mp-Tps	WT	Mp-Tps
Mean	8.92	4.91	7.33	4.54	4.03	3.45
%Mortality	33.4^b	76.7^a	41.5^b	73.4^a	83.9^b	91.4^a
N	58	64	53	63	66	73
R	6	6	6	6	6	6
P-value	—	< 0.0001	—	0.0002	—	0.0002

b

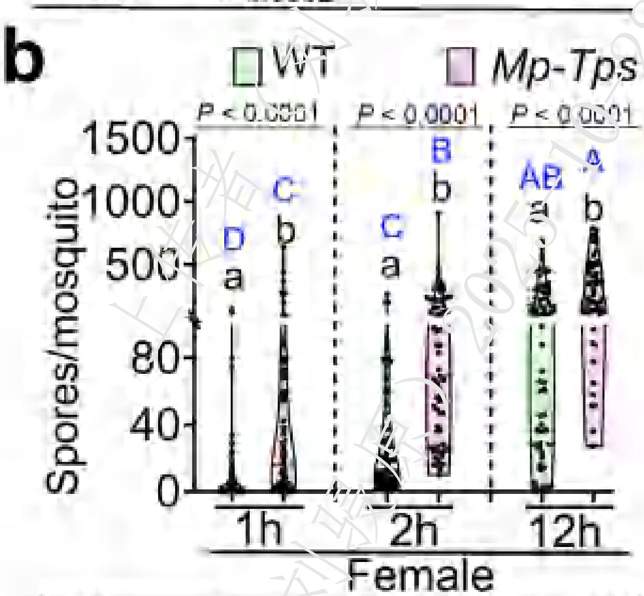

	WT	Mp-Tps	WT	Mp-Tps	WT	Mp-Tps
Mean	75	156	153	250	260	321
Median	1	6	12	69	111	244
%Inoculation	56.2^b	84.3^a	100	100	100	100
N	74	73	67	65	56	56
P-value	---	0.0386	---	---	---	---

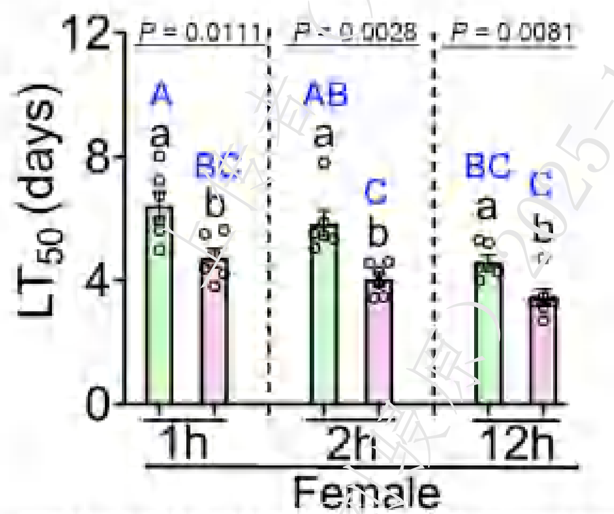

	WT	Mp-Tps	WT	Mp-Tps	WT	Mp-Tps
Mean	6.42	4.73	5.84	4.04	4.60	3.44
%Mortality	50.7^b	78.7^a	62.4^b	84.3^a	87.6^b	93.1^a
N	72	84	77	78	65	74
R	6	6	6	6	6	6
P-value	---	0.0007	---	0.0097	---	0.0431

Extended Data Fig. 8 | The ability of *M. pingshaense* strains to attract and kill laboratory-reared adult *Ae. albopictus* mosquitoes in 1m^3-cages. (**a**) Males. (**b**) Females. WT: the parental WT strain of the transgenic strain *Mp-Tps*. Exposed to *Mp-Tps* or the WT BRH cultures for one (1 h), two (2 h) and 12 (12 h) hours. Left panel: inoculum load (Horizontal line: median) and inoculation rate. Right: LT_{50} values and mortality at day seven post-exposure. Data presented as mean ± SE. Within each figure, different capital letters (blue) indicate significant differences ($P < 0.05$) among all treatments. Different small letters (black) indicate significant differences in inoculum load and LT_{50} (*P* value given on the top) and inoculation rate and mortality (*P* values given below) between the WT and *Mp-Tps* following the same exposure period. For inoculum load, the two-tailed Mann-Whitney test was used for comparisons between two samples, and the Kruskal-Wallis test with Dunn's multiple comparisons test was used for multiple samples. For inoculation rate, LT_{50} values and mortality, two-tailed Student's t-test for two samples and one-way ANOVA with Tukey's multiple-comparison test for multiple samples. N: the total number of mosquitoes assayed; R: experiment repeats.

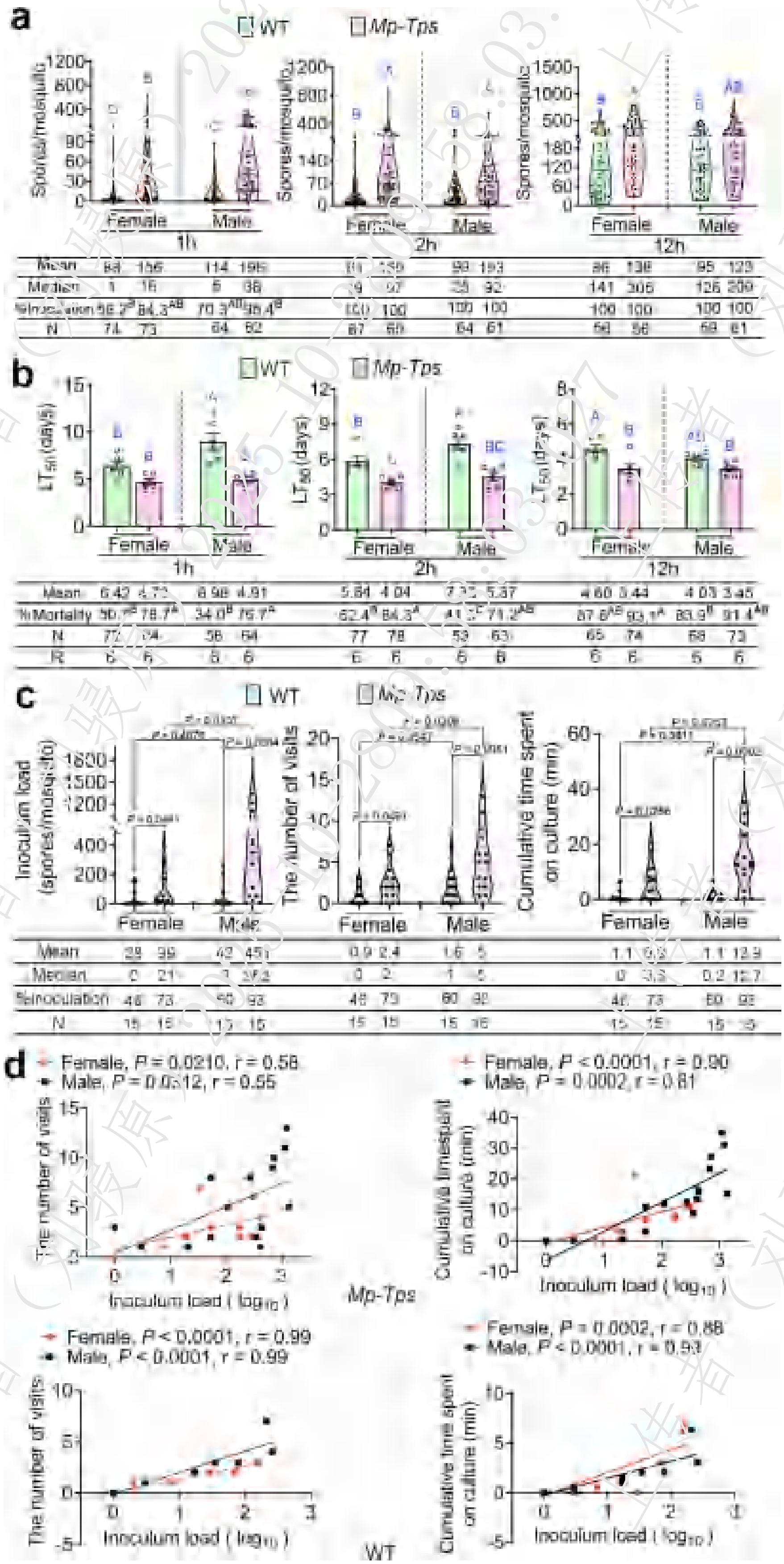

Extended Data Fig. 9 | See next page for caption.

 https://doi.org/10.1038/s41564-025-02155-9

Extended Data Fig. 9 | Differences in infection parameters and visitation to the fungal cultures between female and male mosquitoes. (**a**) The inoculum load (Horizontal line: median) and inoculation rate. WT: the parental WT strain of the transgenic strain *Mp-Tps*. Within the same exposure period, different letters mean significant differences among all treatments ($P < 0.05$, The Kruskal-Wallis test with Dunn's multiple comparisons test). (**b**) LT_{50} values and mortality. Data presented as mean ± SE. Within the same exposure period, different letters mean significant differences among all treatments ($P < 0.05$, one-way ANOVA with Tukey's multiple-comparison test). a and b are other ways to illustrate the data presented in Extended Data Fig. 8. (**c**) Visitation to *Mp-Tps* or the WT BRH cultures (shown as the number of visits and the cumulative time spent on cultures within one hour exposure) and inoculum load during the visitation. Visitation and inoculum load of mosquitoes were individually assayed. Horizontal line: median. N: the number of mosquitoes assayed. Two-tailed Student's t-test was used. (**d**) Correlations between inoculum load per mosquito (log transformation) and the number of visits to fungal cultures (Left) or the cumulative time spent on the cultures (Right). Upper panel: *Mp-Tps* cultures; Lower panel: the WT cultures. Calculations were conducted with the two-tailed Pearson's correlation.

https://doi.org/10.1038/s41564-025-02155-9

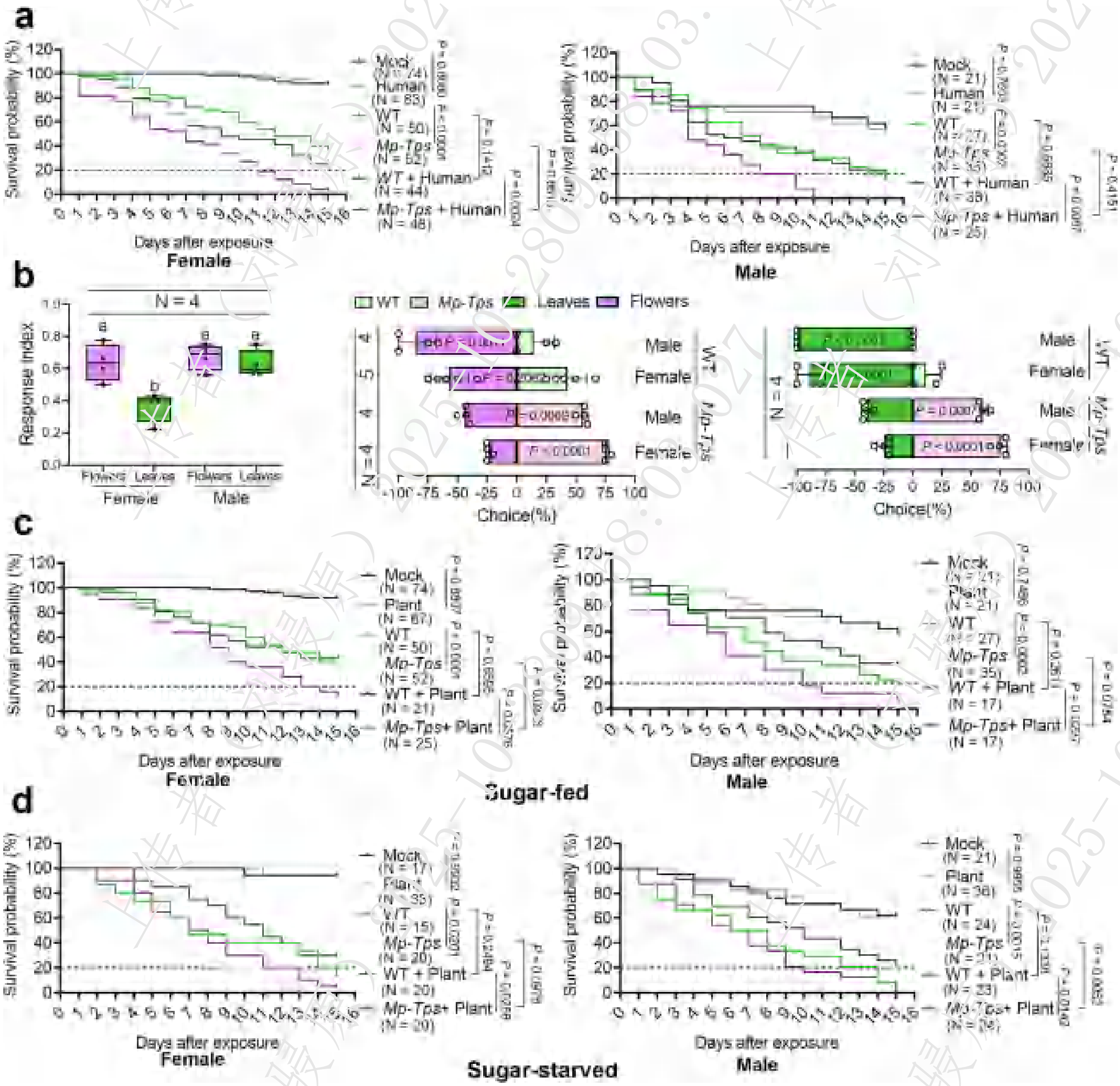

Extended Data Fig. 10 | Impacts of human odors and mosquito-attracting flowering plants on the ability of *Mp-Tps* BRH cultures to attract and kill adult wild-caught *Ae. albopictus* in a large room. This figure supplement Fig. 6. (**a**) Kaplan-Meier curves of survival of mosquitoes treated with the WT and *Mp-Tps* BRH cultures with or without human volunteers. Experiments repeated three to four times. Dashed lines represent 80% mortality (WHO control threshold for successful vector control agent). Mock: untreated mosquitoes; Human: mosquitoes treated with humans only; WT: BRH cultures of the WT strain only; *Mp-Tps*: *Mp-Tps* BRH cultures only; WT + Human: BRH cultures of the WT strain in presence of humans; *Mp-Tps* + Human: *Mp-Tps* BRH cultures in presence of humans; WT + Plant: BRH cultures of the WT strain in presence of plants; *Mp-Tps* + plant: *Mp-Tps* BRH cultures in presence of plants. Log-rank test was used (N: the number of mosquitoes assayed). (**b**) Two-port olfactometer assays of mosquito's response to flowers, leaves, *Mp-Tps* and the WT BRH cultures. Left panel: plant tissues versus water-soaked cotton (control). The box plots show the median (center line), the interquartile range (box bounds, 25th to 75th percentiles), and the whiskers (minima and maxima within 1.5 × interquartile range from the box). Values with different letters are significantly different ($P < 0.05$, one-way ANOVA with Tukey's multiple-comparison test). Response index was calculated as (O-C)/T, where O was the number of mosquitoes in the plant tissue chamber, C was the number in the cotton chamber, and T was the total number of mosquitoes assayed. Middle panel: *Mp-Tps* or the WT BRH cultures versus flowers, and leaves (Right panel). Data presented as mean ± SE. Two-tailed Student's t-test was used. Kaplan-Meier curves of survival of sugar fed (**c**), and (**d**) sugar-starved mosquitoes treated with *Metarhizium* cultures with or without plants.

nature portfolio

Corresponding author(s): Weiguo Fang
Last updated by author(s): September 2, 2025

Reporting Summary

Nature Portfolio wishes to improve the reproducibility of the work that we publish. This form provides structure for consistency and transparency in reporting. For further information on Nature Portfolio policies, see our Editorial Policies and the Editorial Policy Checklist.

Please do not complete any field with "not applicable" or n/a. Refer to the help text for what text to use if an item is not relevant to your study. For final submission: please carefully check your responses for accuracy; you will not be able to make changes later.

Statistics

For all statistical analyses, confirm that the following items are present in the figure legend, table legend, main text, or Methods section.

n/a	Confirmed	
☐	☑	The exact sample size (n) for each experimental group/condition, given as a discrete number and unit of measurement
☐	☑	A statement on whether measurements were taken from distinct samples or whether the same sample was measured repeatedly
☐	☑	The statistical test(s) used AND whether they are one- or two-sided *Only common tests should be described solely by name; describe more complex techniques in the Methods section.*
☐	☑	A description of all covariates tested
☐	☑	A description of any assumptions or corrections, such as tests of normality and adjustment for multiple comparisons
☐	☑	A full description of the statistical parameters including central tendency (e.g. means) or other basic estimates (e.g. regression coefficient) AND variation (e.g. standard deviation) or associated estimates of uncertainty (e.g. confidence intervals)
☐	☑	For null hypothesis testing, the test statistic (e.g. F, t, r) with confidence intervals, effect sizes, degrees of freedom and P value noted *Give P values as exact values whenever suitable.*
☑	☐	For Bayesian analysis, information on the choice of priors and Markov chain Monte Carlo settings
☑	☐	For hierarchical and complex designs, identification of the appropriate level for tests and full reporting of outcomes
☐	☑	Estimates of effect sizes (e.g. Cohen's d, Pearson's r), indicating how they were calculated

Our web collection on statistics for biologists contains articles on many of the points above.

Software and code

Policy information about availability of computer code

Data collection	SSR signals visualized by Autospike v.3.9 software
Data analysis	GraphPad Prism 7.0 for all statistical tests; CytExpert Software 2.4 for flow cytometry; EAG Pro software for EAG signal; GcEad-1.2.5 software for GC-EAD signal

For manuscripts utilizing custom algorithms or software that are central to the research but not yet described in published literature, software must be made available to editors and reviewers. We strongly encourage code deposition in a community repository (e.g. GitHub). See the Nature Portfolio guidelines for submitting code & software for further information.

Data

Policy information about availability of data

All manuscripts must include a data availability statement. This statement should provide the following information, where applicable:

- Accession codes, unique identifiers, or web links for publicly available datasets
- A description of any restrictions on data availability
- For clinical datasets or third party data, please ensure that the statement adheres to our policy

All data are available in the main text or the supplementary materials. The codon-optimized sequence of the pine longifolene synthase TPS was deposited in GenBank (accession number OQ242380).

Research involving human participants, their data, or biological material

Policy information about studies with human participants or human data. See also policy information about sex, gender (identity/presentation), and sexual orientation and race, ethnicity and racism.

Reporting on sex and gender	Two male huamn volunteers used
Reporting on race, ethnicity, or other socially relevant groupings	Two young Chinese males (22 and 25 year old, respectively)
Population characteristics	Not relevant in this study
Recruitment	Two volunteers were randomly selected based on the Ethics Committee approved procedures without any bias that could impact results.
Ethics oversight	The usage of human volunteers in this study was approved (AP code: JIPD-2023-015) by the Ethics Committee of Jiangsu Institute of Parasitic Diseases. A blank informed consent was provided in the article. Signed informed consents had been obtained from the two volunteers.

Note that full information on the approval of the study protocol must also be provided in the manuscript.

Field-specific reporting

Please select the one below that is the best fit for your research. If you are not sure, read the appropriate sections before making your selection.

☑ Life sciences ☐ Behavioural & social sciences ☐ Ecological, evolutionary & environmental sciences

[illegible] mmary-flat.pdf

Life sciences study design

All studies must disclose on these points even when the disclosure is negative.

Sample size	[illegible] For GC-MS analysis, at least 3 biological repeats were used. For SSR, EAG and GC-EAD assays, [illegible] biological repeats were used. [illegible]
Data exclusions	No data were excluded from the analysis
Replication	Sufficient experiment repeats (at least three biological repeats) were conducted to verify reproducibility. Successful replications were confirmed.
Randomization	Randomization was not relevant to this study as samples were not allocated to experimental groups.
Blinding	Binding was not relevant in this study.

Behavioural & social sciences study design

All studies must disclose on these points even when the disclosure is negative.

Study description	
Research sample	
Sampling strategy	
Data collection	
Timing	
Data exclusions	
Non-participation	
Randomization	

Ecological, evolutionary & environmental sciences study design

All studies must disclose on these points even when the disclosure is negative.

Study description	
Research sample	
Sampling strategy	
Data collection	
Timing and spatial scale	
Data exclusions	
Reproducibility	
Randomization	
Blinding	

Did the study involve field work? ☐ Yes ☐ No

Field work, collection and transport

Field conditions	N/A
Location	
Access & import/export	
Disturbance	

Reporting for specific materials, systems and methods

We require information from authors about some types of materials, experimental systems and methods used in many studies. Here, indicate whether each material, system or method listed is relevant to your study. If you are not sure if a list item applies to your research, read the appropriate section before selecting a response.

Materials & experimental systems

n/a	Involved in the study	
☑	☐	Antibodies
☑	☐	Eukaryotic cell lines
☑	☐	Palaeontology and archaeology
☐	☑	Animals and other organisms
☑	☐	Clinical data
☐	☑	Dual use research of concern
☐	☑	Plants

Methods

n/a	Involved in the study	
☑	☐	ChIP-seq
☐	☑	Flow cytometry
☑	☐	MRI-based neuroimaging

Antibodies

Antibodies used	
Validation	

Eukaryotic cell lines

Policy information about cell lines and Sex and Gender in Research

Cell line source(s)	
Authentication	
Mycoplasma contamination	
Commonly misidentified lines (See ICLAC register)	

Palaeontology and Archaeology

Specimen provenance	
Specimen deposition	
Dating methods	

☐ Tick this box to confirm that the raw and calibrated dates are available in the paper or in Supplementary Information.

Ethics oversight	

Note that full information on the approval of the study protocol must also be provided in the manuscript.

Animals and other research organisms

Policy information about studies involving animals; ARRIVE guidelines recommended for reporting animal research, and Sex and Gender in Research

Laboratory animals	Insects used include mosquitoes, Drosophila melanogaster, Galleria mellonella, adult wasp Leptopilina boulardi, adult cotton mealybug Phenacoccus solenopsis and whitefly Bemisia tabaci.
Wild animals	Wild-caught Aedes albopictus mosquitoes
Reporting on sex	Provided
Field-collected samples	Wild-caught Ae. albopictus mosquitoes
Ethics oversight	Not relevant

Note that full information on the approval of the study protocol must also be provided in the manuscript.

Clinical data

Policy information about clinical studies

All manuscripts should comply with the ICMJE guidelines for publication of clinical research and a completed CONSORT checklist must be included with all submissions.

Clinical trial registration	
Study protocol	
Data collection	
Outcomes	

Dual use research of concern

Policy information about dual use research of concern

Hazards

Could the accidental, deliberate or reckless misuse of agents or technologies generated in the work, or the application of information presented in the manuscript, pose a threat to:

No	Yes	
☑	☐	Public health
☑	☐	National security
☑	☐	Crops and/or livestock
☑	☐	Ecosystems
☑	☐	Any other significant area

Experiments of concern

Does the work involve any of these experiments of concern:

No	Yes	
☑	☐	Demonstrate how to render a vaccine ineffective
☑	☐	Confer resistance to therapeutically useful antibiotics or antiviral agents
☑	☐	Enhance the virulence of a pathogen or render a nonpathogen virulent
☑	☐	Increase transmissibility of a pathogen
☑	☐	Alter the host range of a pathogen
☑	☐	Enable evasion of diagnostic/detection modalities
☑	☐	Enable the weaponization of a biological agent or toxin
☑	☐	Any other potentially harmful combination of experiments and agents

Plants

Seed stocks	Mexican petunia plants purchased from local markets
Novel plant genotypes	Not relevant in this study
Authentication	Not relevant in this study

ChIP-seq

Data deposition

☐ Confirm that both raw and final processed data have been deposited in a public database such as GEO.

☐ Confirm that you have deposited or provided access to graph files (e.g. BED files) for the called peaks.

Data access links May remain private before publication.	
Files in database submission	
Genome browser session (e.g. UCSC)	

Methodology

Replicates	
Sequencing depth	
Antibodies	
Peak calling parameters	
Data quality	
Software	

Flow Cytometry

Plots

Confirm that:

☑ The axis labels state the marker and fluorochrome used (e.g. CD4-FITC).

☑ The axis scales are clearly visible. Include numbers along axes only for bottom left plot of group (a 'group' is an analysis of identical markers).

☑ All plots are contour plots with outliers or pseudocolor plots.

☑ A numerical value for number of cells or percentage (with statistics) is provided.

Methodology

Sample preparation	Fungal spores
Instrument	Flow Cytometry (Beckman Coulter, USA)
Software	CytExpert Software 2.4
Cell population abundance	50,000 spores
Gating strategy	FITC

☑ Tick this box to confirm that a figure exemplifying the gating strategy is provided in the Supplementary Information.

Magnetic resonance imaging

Experimental design

Design type	
Design specifications	
Behavioral performance measures	
Imaging type(s)	
Field strength	
Sequence & imaging parameters	
Area of acquisition	

Diffusion MRI ☐ Used ☐ Not used

Preprocessing

Preprocessing software	
Normalization	
Normalization template	
Noise and artifact removal	
Volume censoring	

Statistical modeling & inference

Model type and settings	
Effect(s) tested	

Specify type of analysis: ☐ Whole brain ☐ ROI-based ☐ Both

Statistic type for inference

(See Eklund et al. 2016)

Correction

Models & analysis

n/a	Involved in the study
☐	☐ Functional and/or effective connectivity
☐	☐ Graph analysis
☐	☐ Multivariate modeling or predictive analysis

Functional and/or effective connectivity

Graph analysis

Multivariate modeling and predictive analysis